Chapter 3
Performance Evaluation and Traffic Modeling

Hans van den Berg, Thomas M. Bohnert, Orlando Cabral, Dmitri Moltchanov, Dirk Staehle, and Fernando Velez

3.1 Introduction

Mobile and wireless communication systems are becoming more and more complex, making understanding the interaction of different technologies on different layers a very difficult task. The introduction of sophisticated techniques on the physical layer that react to changes of the wireless channel on small timescales requires new paradigms for modeling, simulating, and analyzing current and future wireless networks. Investigating the relationship of new physical layer techniques, application-specific requirements and performance measures will become a major research topic for future wireless networks. A continuous change in the methodology for evaluating the network performance takes place in the Internet. In the past, network performance was mainly evaluated using concretely measurable values like packet loss rate, delay, or jitter. The current trend in the Internet goes toward application-specific quality measures that judge more the subjective experience of the end user than they do network parameters. In the terminology, this is expressed as the change from quality of service (QoS) to quality of experience (QoE). For wireless networks this leads to interesting consequences, as currently the traffic requirements for MAC layer connections are mainly formulated in terms of QoS parameters. Accomplishing the change from QoS to QoE also in the definition of connection parameters is a future challenge for wireless networks, for which the first approaches are presented.

This chapter covers all issues related to performance evaluation and traffic modeling of mobile and wireless networks. As such, the main focus is on the development of novel techniques for modeling and evaluation of already existing technologies and concepts for current and future wireless networks. As a consequence, Chapter 3 can be seen as complementary to Chapter 2, "Packet Scheduling and Congestion Control," where the focus is on the development and enhancement of wireless network technologies.

H. van den Berg (✉)
TNO, The Netherlands
e-mail: j.l.vandenberg@telecom.tno.nl

Y. Koucheryavy et al. (eds.), *Traffic and QoS Management in Wireless Multimedia Networks*, Lecture Notes in Electrical Engineering 31,
DOI 10.1007/978-0-387-85573-8_3, © Springer Science+Business Media, LLC 2009

Performance evaluation comes with different facets: the first one is the development of simulation tools and analytic models in order to determine the performance or capacity of mobile and wireless systems on a detailed or abstract level. The development of performance evaluation methodology and traffic models is the basis for the development of radio resource management strategies, network planning, and parameterization. Section 3.1 will give an overview of the models developed with the COST Action 290. Models dealing with flow-level performance are presented in Section 3.2.1, and Section 3.2.2 focuses on packet-level models.

A second facet of performance evaluation is the use of simulation models or measurement campaigns in either real network environments or laboratory testbeds in order to evaluate certain performance measures of an existing or future radio network technology. Section 3.3 presents simulation models for performance evaluation on both link and system level. Setup and results from real network measurements concerning TCP traffic are also presented.

In today's wireless multiservice network carrying a large variety of different applications, the evaluation of the user-perceived quality of service plays an increasingly important role. Simple network statistics like packet loss, delay, or jitter alone are not sufficient to judge the quality that a user actually experiences. Section 3.4 describes how to assess the quality experienced by a user and how to use this information for resource or source control.

Radio network planning relies strongly on good and fast models for evaluating the quality of a network layout. The optimization of base station sites and the individual site configuration in an advanced radio access network like UMTS is very complex and typically solved by iteratively improving the network configuration. The time for judging the quality of a network configuration determines the number of configurations that can be tested. The accuracy of the evaluation of a network configuration determines how well the final solution will meet the actual network needs and also how straightforward the disadvantages of a configuration can be mitigated in the next iteration step. Section 3.4 focuses on coverage planning for broadband wireless access networks including experiences from a practical network setup in Portugal.

3.2 Traffic Modeling

This section covers traffic modeling issues in mobile and wireless networks. The section is subdivided into two parts. The first part presents models for evaluating the impact of flow-level traffic dynamics in large-scale wireless networks. The second part addresses the dynamics on the packet level and focuses on the properties of a single wireless link.

From a technological point of view, the focus is on *Universal Mobile Telecommunication System* (UMTS), as it is the predominant European mobile network technology during the course of the Action. The UMTS enhancements

High Speed Downlink Packet Access (HSDPA) and *Enhanced Uplink* or *High Speed Uplink Packet Access* (HSUPA) brought new challenges for UMTS traffic models because they are the first really packet-switched cellular technologies. Beside the technology centric models on cellular UMTS, quite generic models applicable to various radio technologies are also presented.

3.2.1 System and Flow-Level Modeling

The performance of mobile and wireless networks depends on the time-varying nature of the wireless channel and on the different protocols working on physical and *Medium Access Control* (MAC) layer in order to compensate for or even utilize the time-varying nature of the wireless channel. Among the most prominent of these techniques, we have fast power control, *adaptive modulation and coding* (AMC), *hybrid automatic repeat request* (H-ARQ), channel-aware scheduling, and many more. Common to all these techniques is that they have a considerable impact on the system performance and take place at very small timescales of the order a few microseconds or even less. On the other hand, obtaining statistically significant results about the performance on system or flow level such as blocking probabilities, average throughput, or transfer times requires considering large networks for a long time, making detailed simulation very time-consuming or inapplicable. A convenient technique for obtaining results in acceptable timescales is to use analytic models or abstract simulation models on flow level that use an intelligent algorithm for determining the system behavior between flow-level events such as arrivals, departure, or activity changes. This section follows the development of UMTS during the past years by first looking at Release 99 downlink, then at the HSDPA introduced in Release 5, and finally at the Enhanced Uplink introduced in Release 6. The work on UMTS is followed by two contributions without close technological relationship presenting models for flow-level performance analysis of multi-access and multihop networks. The section is concluded by a contribution on the evaluation of service-level architectures in mobile networks.

3.2.1.1 UMTS Evolution

The quality of a UMTS radio network is judged by its ability to serve all users where they are and with the desired and appraised quality. This means that both coverage area and capacity of the network must be sufficient. The coverage area is typically limited by the uplink, as the *user equipment* (UE) power is much lower than the Node-B power. The capacity limitation depends strongly on the underlying services. In a voice-only network with symmetric traffic demands, the limiting factor will be the uplink. Consequently, the uplink was the major research focus at the time of narrow-band *Code Division Multiple Access* (CDMA) networks such as IS95 [Vit93, Vee97, Eva99]. This changed with the introduction of *Wideband CDMA* (WCDMA) in UMTS networks. Internet

access envisaged as one of the key services produced heavily asymmetric traffic, with an unbalance factor of up to 75 for large file transfers.

Downlink Capacity of Release 99 UMTS Networks

The downlink capacity is limited by the Node-B transmit power, which comprises a constant part spent for signaling and common channels and a variable part for *dedicated channels* (DCH). After the introduction of HSDPA, a considerable part is also spent for the *high-speed downlink shared channel* (HS-DSCH), which is dealt with in more detail in the next section. The power of a dedicated channel depends on the interference at and the propagation loss to the location of the user. In the center of the cell, close to the base station, the interference is dominated by the own-cell interference, which is caused by multipath propagation. The orthogonality factor model approximates the own-cell interference as a fixed fraction of the total received own-cell power. At the cell border, the other-interference becomes dominating, and per interfering cell exceeds the own-cell interference by the reciprocal of the orthogonality factor if we assume equal transmit powers.

The difficulty in computing the required transmit power and as such the capacity of a network lies in capturing the impact of the other-cell interference correctly. Quite basic models [Hil00, Sip00] introduce a factor characterizing the other-cell load as a fraction of the own-cell load similar to the model of [Vit94] for the uplink. The advantage of this approach is its simplicity. The drawback of the approach is its limitation to hexagonal cell layouts and homogeneous traffic distributions, and in particular its impotence to capture the effect of traffic dynamics . In [Sta04, TD(04)002], an approach is presented to determine mean and variance of the transmit power required by the DCHs of a Node-B or a sector in a UMTS network. The mutual relationship of cell transmit powers is taken into account by formulating and solving matrix equations for both mean and variance of the Node-B transmit powers in a network. The distribution of DCH transmit powers is assumed to be lognormal and is as such entirely characterized by its mean and variance. That allows estimating the probability that the maximum sustained transmit power of a Node-B is exceeded and a cell is in outage.

The model is applied to a network with arbitrarily chosen Node-B sites and heterogeneous traffic distribution. The network is depicted in Fig. 3.1 with darker colors indicating higher traffic intensities. The validation of the model through extensive Monte Carlo simulations as illustrated in Fig. 3.2 shows that the method is capable of deriving mean and standard deviation of the Node-B transmit powers with an accuracy of more than 90%.

High Speed Packet Downlink Access

The HSDPA was introduced in UMTS Release 5. It is specially designed for an efficient support of mobile Internet access with packet-switched data. Typical

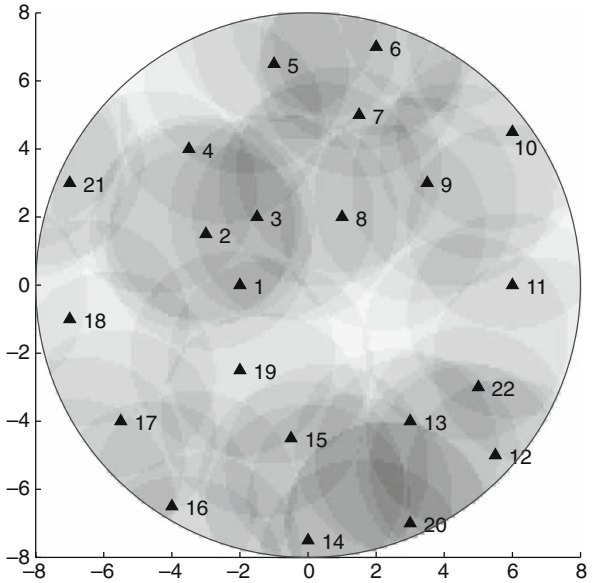

Fig. 3.1 Example network (copyright © 2005 IEEE [Sta05])

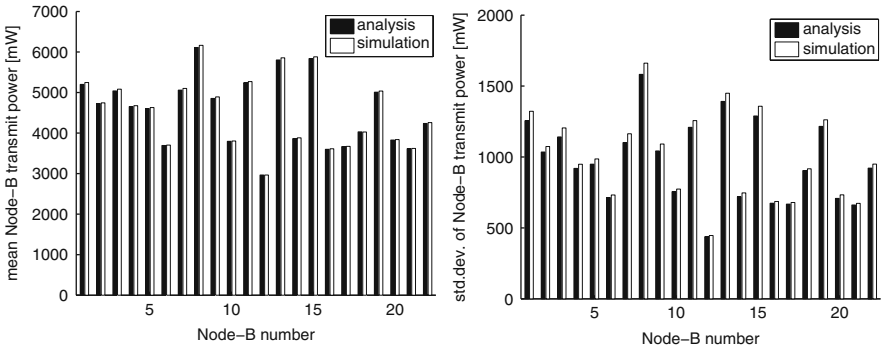

Fig. 3.2 Model shows very accurate results (copyright © 2007 IEEE [Sta04])

Internet usage produces bursty traffic with short periods of high bandwidth demand and long periods with no data to transmit. On the downlink, this causes the problem that a user continuously occupies a DCH with its associated channelization code though no data is transmitted (i.e., the activity factor is very low). As shown in [Sta05, TD(06)026], low activity factors lead to a limitation of the cell capacity by the available channelization codes and not by the multiple access interference that is desired because that corresponds with an efficient usage of spectrum. In order to shift the capacity limitation from

code-limited to interference-limited, the average power per code needs to be increased. This can be achieved by increasing the activity factor or by increasing the amount of data transmitted per code by introducing higher modulation schemes or using less robust coding. The main feature of HSDPA is that the connections to multiple mobiles are time-multiplexed on one or more channels with fixed spreading factor. This leads to a high activity and consequently to a high code utilization.

The main features of the HSDPA are AMC, packet- scheduling with time and code-multiplex, H-ARQ, and short *transmission time intervals* (TTI) of 2 ms. AMC and opportunistic scheduling are enabled by a feedback channel that is used by the mobiles to report their channel quality expressed by the *Channel Quality Identifier* (CQI) to the Node-B. The *Transport Format and Resource Combination* (TFRC) relates the CQI to the *Transport Block Size* (TBS), the number of parallel codes, and the reference power adjustment. In [25.214], TFRCs for different UE classes are specified. Indirectly, the TRFCs also define the coding rate and modulation scheme to be used. Accordingly, a mobile has to estimate its channel quality and map it to the right CQI. In general, this is a quite complicated task as a certain channel prediction is necessary to compensate for the feedback delay. Opportunistic scheduling allows the Node-B to consider the CQIs reported from different mobiles (see Section 2.2.1 in Chapter 2 for different scheduling schemes). H-ARQ enables a secure communication with rather low *Signal-to-Interference Ratio* (SIR) values by soft-combining retransmissions with prior transmission. According to [Bro04], the first transmission aims at a frame error rate of 10%.

HSDPA performance is typically investigated by means of packet-level simulations of *persistent* [Ber02, Ber03] or *semipersistent* [Fur02, Lov01] data flows, where a given number of terminals maintain endless Web browsing sessions, considering the aggregate performance impact of all relevant system and environment aspects in detailed simulation models and not capturing the true flow-level dynamics. The term *flow-level dynamics* refers to the initiation and completion of (finite) flows at various locations, leading to a varying number of concurrent flows competing for shared resources. On the other hand, analytical *flow-level* performance evaluation approaches are generally forced to consider rather idealistic models [Bon03a, Bor03].

The Impact of Key System and Traffic Aspects

The following section intends to provide deeper insight by decomposing the flow-level performance induced by different scheduling schemes in a UMTS/HSDPA network with respect to the relative performance impact of a set of key system, environment, and traffic-related aspects. In particular, the focus lies on the impact of terminal location, the presence of multipath fading and intercellular interference, the inherent feedback delay in the channel quality reports, the correctional capabilities of HSDPA's H-ARQ scheme, the flow-level traffic

dynamics, and the flow-size variability. In order to investigate these impacts, both analytical models and a detailed system simulator have been developed.

In [Ber04, TD(05)007], the authors consider a 19-cellular UMTS/HSDPA network of omnidirectional Node-Bs in a wraparound hexagonal layout with 1 km Node-B distance. Downlink data transfers of an exponential data volume with 320 kbit in mean are initiated according to a homogeneous spatial Poisson process. Three distinct packet schedulers are considered: the channel-oblivious *Round Robin* (RR) scheme and two channel-aware schemes, in particular the pure *Signal-to-Noise Ratio* (SNR)-based scheduler and the *Proportional Fair* (PF) scheduler. The RR scheduler cyclically serves the current data flows with a TTI heartbeat and is thus intrinsically fair in the sense that each data flow gets an egalitarian share of the HS-DSCH resources. The SNR-based scheduler bluntly exploits the channel quality variations due to multipath fading, in the sense that in each TTI it serves the data flow with the most favorable instantaneous channel conditions. Thus, it greedily maximizes the instantaneous system throughput at the expected cost of a reduced fairness among data flows, as near UEs are more likely to be served than remote ones. The PF scheduler aims to strike a compromise between the fairness of the RR scheme and the efficiency of the SNR-based scheduler by serving that flow at TTI t that maximizes the ratio $R_m(t)/R'_m(t)$, where $R_m(t)$ denotes the instantaneous gross data rate of flow m, and $R'_m(t)$ denotes its exponentially smoothed experienced gross data rate.

Considering both a single cell and a network scenario, for each of the three packet scheduling schemes the expected flow transfer times will be determined as a function of the terminal location, for four distinct gradually more complete (realistic) scenarios that are specified in the table below. The experiments are thus explicitly targeted to reveal the performance impact of the terminals' distance to the serving Node-B, the presence of intercellular interference, the presence of multipath fading, the CQI feedback delay, H-ARQ functionality, and the applied packet scheduling scheme.

The scenarios shown in Table 3.1 have been evaluated using analytical modeling and analysis (for Scenarios I to II) and detailed system simulations (Scenarios I to IV). The analytical modeling is based on dividing each cell area into n disjoint zones with growing distance to the base station. In particular, for the single cell case, the resulting system with RR scheduling and zone-specific bit transfer rates r_j can be modeled by an M/G/1 processor sharing queuing model with n flow classes. This model is analytically tractable and yields

Table 3.1 Overview of scenario parameters

	Multipath Fading	CQI Delay	ARQ
Scenario I	No	Ideal	Basic
Scenario II	Yes	Ideal	Basic
Scenario III	Yes	3 TTIs	Basic
Scenario IV	Yes	3 TTIs	H-ARQ

insightful explicit formulas for the system performance. For example, the expected transfer time of a flow to a user in zone j is derived to be equal to:

$$E[T_j] = \frac{1/(r_j \mu)}{1-\rho}, \tag{3.1}$$

where $1/\mu$ denotes the mean flow size (in bits) and ρ the total traffic load offered to the system. Numerical results (obtained from the analytical model and from the simulations) for each of the three scheduling schemes are shown in the graphs of Fig. 3.3.

The main observations and conclusions from the numerical study are as follows: The presence of multipath fading has a positive effect on the flow-level performance, in particular under channel-aware schedulers. The CQI feedback delay causes severe performance degradation. An increased number of block errors due to the CQI feedback delay can be partially coped with by H-ARQ reducing the negative effect of the CQI delay considerably. Overall, the pure SNR-based scheduler outperforms the other considered schedulers (including the well-known PF scheduler!) with respect to the absolute transfer time performance and the spatial fairness regarding transfer times. Finally, it is noted that for the scenarios where the analytical modeling can be applied, its results correspond very well with the results obtained from detailed system simulations. Besides considering mean flow transfer times, the extent up to which various system and traffic aspects contribute to the variability of the flow-transfer times was also investigated. Please refer to [Ber04] for a detailed description of the setup of this study and the main results. An extension of the analytic modeling approach to the multiple-cell case and SNR-based scheduling is also found there.

Abstraction Model for the HSDPA MAC and Physical Layer

As described above, performance evaluation for HSDPA is mostly based on detailed packet-level simulations or quite abstract simulation models not capable of capturing the impact of physical and MAC layer. In the previous section, a flow-level simulation model based on data rates per zones obtained from link-level simulations was presented and the impact of different scheduling schemes was investigated. In this section, summarizing [Sta07, TD(07)001], a simple model for deriving the data rate at a certain location is presented. Staehle and Mäder address the problem how to compute the data rate of HSDPA users in a certain static network situation. The network consists of a set of Node-Bs and a set of mobiles that either use DCHs or the HSDPA. The problem in time-dynamic flow-level simulations is how to determine the amount of data that HSDPA users transmit in a certain period of time during which the assumption can be made that the system experiences constant shadowing, and constant but different transmit powers for all Node-Bs can be assumed. After that period, users might move to new locations, new users might

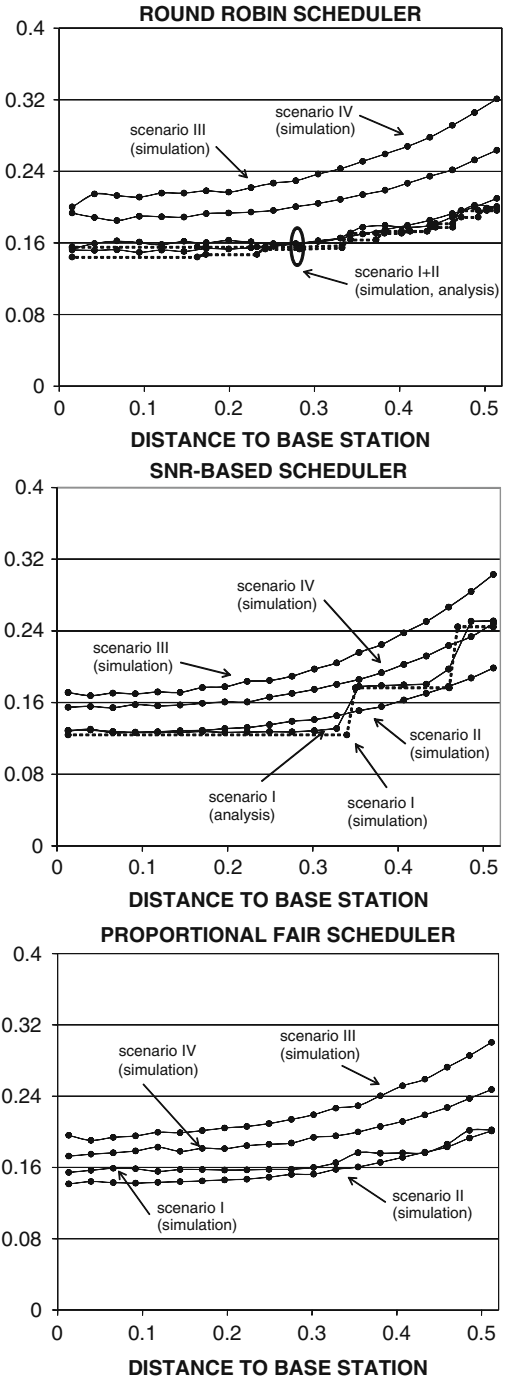

Fig. 3.3 Numerical results for the various scenarios, for each of the three considered scheduling schemes (copyright © 2004 ACM [Ber04])

appear, and some users might leave the system according to the data they transmitted. Then, the data volume transmitted in the next time period can be determined for the new situation.

A simple and computationally efficient algorithm is provided for estimating the probability distribution of the CQI in a static network situation. The CQI distribution allows determining the bandwidth of the HSDPA users under consideration of the available codes and the UE classes for different scheduling disciplines. Whereas [Sta07] focuses on the simplest one, round-robin scheduling, an extension to further scheduling schemes can be found in [Mäd07].

The well-accepted models for the downlink capacity of WCDMA systems [Hil00, Sip00, Sta04] introduce the orthogonality factor to describe the own-cell interference that results from multipath propagation . In analytic or abstract simulation models, this orthogonality factor α is used as a constant that assumes values between 0.05 and 0.4, which means that a share α of the power received from the own-cell is seen as interference.

This model is well-suited and generally accepted to model the average own-cell interference for DCHs. In reality, however, the orthogonality factor is no constant but a fast-varying value that depends on the multipath propagation, both from the own and – if the user is located close to the cell edge – also from the surrounding Node-Bs.

The intrinsic idea of the orthogonality factor model is to approximate the mean signal-to-interference ratio as a one-parametric function of the ratio of mean other-cell received power to mean own-cell received power. This idea is extended to a function that maps the ratio of mean other-cell received power to mean own-cell received power not only to the mean of the SIR but also to the distribution of the SIR. Although the orthogonality factor model allows catching the impact of the multipath channel in a single variable, the orthogonality factor, the function or better algorithm to derive the SIR distribution from the other-to-own-cell interference ratio is more complex. In a first step, four-parametric Weibull functions are found to map the other-to-own-cell interference to the mean and the variance of the SIR. In a second step, different two-parametric distributions are fitted to the SIR distribution in linear and decibel scale, and the Normal distribution for the SIR in decibel scale is identified as best suited.

Figure 3.4 demonstrates the accuracy but also the approximation character of the approach. In left graphic we see the standard deviation of the SIR in dependence of the other-to-own-cell received power ratio. The small dots represent the results from Monte Carlo simulations in very generally defined networks. The solid lines show the fitted four-parametric Weibull functions. We observe that the dots are scattered around the solid lines. This indicates that the standard deviation is not exactly a function of the average other-to-own-cell received power ratio. However, the Weibull functions are located in the center of the dots and match the majority of them quite well. Accordingly, the relation of average other-to-own-cell power ratio and SIR standard deviation possesses a function-like characteristic and can be well approximated by the provided

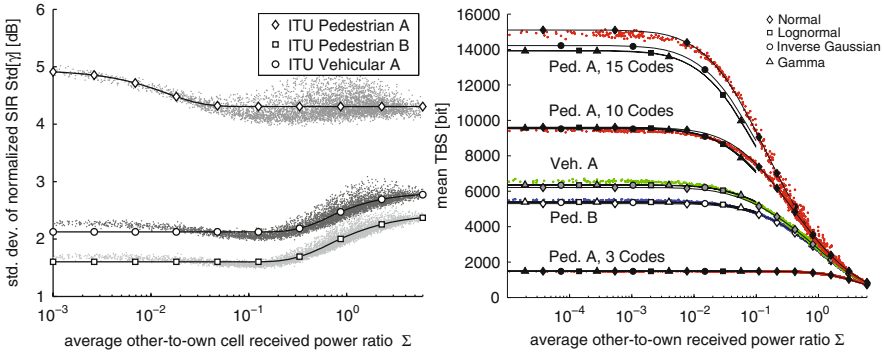

Fig. 3.4 Accuracy of the HSDPA bandwidth model (copyright © 2007 IEEE [Sta07])

Weibull functions. The same plots for the mean SIR show an even more function-like characteristic. The right graphic shows the mean TBS, that is, the mean number of bits transmitted in 2 ms, in dependence of the average other-to-own-cell power ratio. We can observe that in spite of the discernible deviation of the SIR standard deviation, the approximation of the mean TBS is quite accurate.

Enhanced Uplink

The UMTS enhanced uplink is a set of new transport and signaling bearers as well as functional entities introduced in Release 6 of the 3GPP UMTS standard [25.309]. The purpose of the enhanced uplink is to overcome certain limitations of the existing DCH transport bearers if used in conjunction with packet-switched data. Packet-switched data traffic can be roughly categorized as elastic traffic like Web or *Peer-to-Peer* (P2P) traffic, that is, traffic originating from typical best-effort applications and traffic that requires certain QoS guarantees like *Voice over IP* (VoIP), video streaming, or gaming. Whereas DCH bearers are suitable for the transport of QoS traffic, the characteristics of elastic traffic require transport bearers that adapt to the traffic demand to avoid waste of resources. At the same time, elastic traffic also permits the downgrading of existing connections, because they do not have hard QoS requirements that have to be fulfilled.

The enhanced uplink meets these requirements by introducing *Enhanced Dedicated Channels* (E-DCH) with two new main features: shorter TTIs of 2 ms and a flexible resource allocation mechanism that is located mainly in the Node-B. Additional features are H-ARQ and multicode transmissions. An overview of the changes and additional features of the enhanced uplink is provided in [Par05, Hol06b]. The short TTIs and the fast rate control enable fast reactions on variations in traffic demand or resource availability and thus lead to a more efficient resource allocation than in Release 5 or Release 99. The

Node-B–based scheduling introduces a new flexibility into the UMTS air interface, as it enables the vendor or operator to implement a scheduling mechanism that is between two fundamentally different scheduling paradigms: one-by-one scheduling and parallel scheduling. It should be noted, however, that one-by-one scheduling is only a theoretical option because it would require nearly perfect synchronization of the uplink radio bearers.

In [Mäd06, TD(06)006], a performance model for a UMTS network with classic DCH and E-DCH connections in coexistence is proposed. The model considers lognormal-distributed other-cell interference and the influence of fast power control imperfection. Admission control is modeled on the assumption of a certain guaranteed minimum data rate for E-DCH users. Figure 3.5 shows the mean user throughput versus the total arrival rate for parallel (par) and one-by-one (obo) scheduling and different minimum guaranteed data rates R_{min} of 60 kbit/s and 200 kbit/s. One-by-one scheduling leads to better results due to the lack of own-cell interference. Higher minimum data rates lead to higher throughputs as well, although this advantage is paid for by higher blocking probabilities. With higher loads, the gain of one-by-one over parallel scheduling shrinks because of the increasing number of DCH connections that have a higher priority than do E-DCH connections.

3.2.1.2 Transmit Diversity in Multiaccess Networks

Radio access networks in personal communication systems today generally either operate on a single radio interface or integrate multiple radio interfaces at flow level. In addition to such flow-level cooperation, the different *radio*

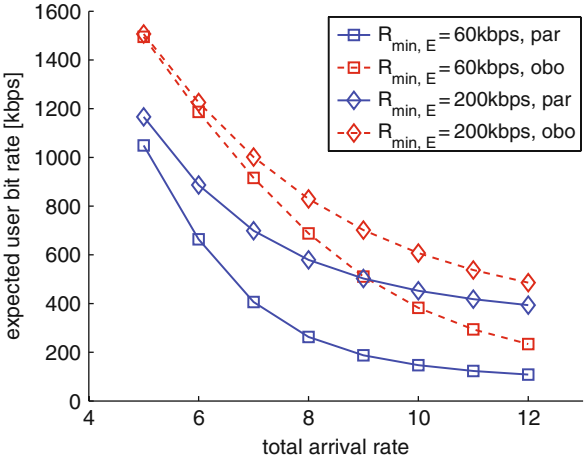

Fig. 3.5 User data rates for different scenarios (copyright © 2006 IEEE [Mäd06])

accesses (RAs) could in principle be more tightly integrated, enabling access coordination at a packet (or frame) level.

In such integrated networks, both RA selection and multiaccess packet scheduling become key radio resource management mechanisms that strongly affect service quality and network capacity. With regard to RA selection and scheduling, two distinct forms of diversity are envisaged. On one hand, multiuser diversity stems from the fact that a channel-aware scheduler opportunistically time-multiplexes multiple data flows over a single shared transport channel, always selecting the flow with the most favorable current (relative) channel conditions. On the other hand, *Multi-Radio Transmit Diversity* (MRTD) stems from the fact that a channel-aware RA selection scheme opportunistically chooses between multiple RAs when serving a given data flow, again always assigning the RA with the most favorable conditions. Both types of diversity enhance throughput performance.

Aside from the identified diversity gains, the integration of multiple RAs yields a trunking gain, which stems from the generic observation that an L times increase in the capacity yields an above-L times increase in the supportable traffic load, given some performance target (e.g., a maximum average transfer time or blocking probability). The significance of the trunking gain, which is due to flow-level multiplexing, is readily observed from traditional queuing models for single RA systems (e.g., the Erlang loss model or the processor sharing model).

In [Ber06, TD(06)027], a purely analytical integrated packet/flow-level performance model is presented for tightly integrated multiaccess networks involving opportunistic RA selection and packet scheduling. At packet level, a persistent flow analysis is presented to capture the channel-oblivious or channel-aware access selection and scheduling operations at a small timescale, whereas a non-persistent flow analysis captures the flow-level dynamics that is due to the initiation and completion of finite flows.

Applying the model and analysis, the included numerical experiments demonstrate the (relative) significance of the diversity and trunking gains. From these experiments, it is concluded that the exploitation of multiuser/multiradio transmit diversity with a channel-aware access selection scheme attains the most significant gains, while also the trunking gain, which is due to an above-proportional performance enhancement when aggregating system-specific capacities, is noted to be significant. Although parallel MRTD, where multiple RAs may be assigned to a given flow, demonstrated enhancement of peak rates in light traffic scenarios, in general the achieved benefits appeared to be rather limited when compared with the implementationally less complex alternative of switched MRTD, where a single flow may be assigned no more than a single RA at a time. Applying a slightly different perspective, the derived results have been argued to also allow an assessment of the performance difference between scenarios with isolated versus integrated radio access networks, which has been demonstrated to be particularly significant when considering flow-level dynamics.

3.2.1.3 Multihop Networks

Flow-level modeling of wireless multihop networks faces two fundamental challenges: the modeling effects of the MAC layer and the modeling effects of the flow-level resource sharing. (Please refer also to Chapter 5 for a deeper discussion of wireless multihop networks. In particular, Section 5.2.1 is closely related to this section as it presents an alternative way for investigating the multihop network performance for flow-level metrics.) The approach presented in this section in order to gain understanding of flow-level performance provided by a multihop network is to assume that the duration of a MAC-layer time slot is very short compared with the duration of a typical flow. As a result, a flow-level virtual network is obtained where the link capacities are flow-level time averages of the actual link capacities under the MAC protocol/scheduler. The virtual capacities can be adjusted by changing the MAC-layer parameters like the transmission schedule.

At flow level, the traffic consists mainly of file transfers that are elastic by nature. The file transfers (flows) can adapt their transmission rate to share the network resources. Interesting performance measures in data networks like file transfer delays can be analyzed only in a dynamic system, where file transfers are initiated (randomly) and also leave the network upon completion. By modeling the resource sharing by balanced fairness [Bon03b], performance analysis in this dynamic setting becomes more feasible. By combining scheduling and balanced fairness – resource sharing under timescale separation – one can, at least approximately, analyze the flow-level performance of a wireless multihop network. Each time the flow state changes (i.e., when a flow enters or leaves), the bit rates of the flows are determined by balanced fairness up to a common constant. The performance is then optimized by maximizing the constant over the MAC-layer parameters.

In [Lei07, TD(07)022], a slotted Aloha type random access network is considered: each link transmits in each time slot with a certain probability, independently of other links. The link transmission probabilities are tuned at the flow level; every file arrival or departure results in a potential probability update. An optimization algorithm for these probability updates is derived, and a method how to analyze flow throughputs in a multihop random access network is proposed. Conceptually, the work goes one step further: The MAC-layer parameters reduce to a single probability value for each network node (the sum of the outgoing links' probabilities). Now, having only a small number of parameters, which, moreover, have to be updated only on flow timescale (i.e., there is no control traffic per-time-slot basis), an approach called flow-optimized random access appears as an interesting alternative to the per-time-slot scheduling/contention resolution. The latter would require more information and a smaller timescale for optimal implementation. Indeed, performance analyses show that for short routes with low loads, the flow-optimized random access scheme performs almost optimally at flow level (corresponding with centralized per-slot scheduling). However, for heavy load and/or long routes, the performance of the proposed scheme deteriorates.

3.2.1.4 Performance Analysis of Service Architectures in Mobile Networks

One way of increasing the revenue for a mobile operator is to open up its network to third-party service providers. Please note that for reasons of simplicity, the term *service provider* is used instead of *third-party service provider* from now on. The services of service providers can be accessed from a Web page or via a mobile terminal. To facilitate this, a standardized interface between the mobile network's nodes and the service provider's server is needed. The mobile network and the server exchange information needed for a service via a gateway. For example, the service provider may ask for the position of a mobile subscriber or order the mobile network to set up a call. One example of such architectures is the Parlay X architecture (www.parlay.org), which was used as reference architecture in the studies summarized in this section.

In a service architecture, it is important that servers, gateways, *home locations registers* (HLRs), or other processing nodes do not get too heavily loaded by a high requests arrival rate. If that happens, queues will build up and subscribers will experience long waiting times. The nodes might have to be protected by overload control mechanisms that can reject requests if the load is too heavy. Such mechanisms have been used for decades in telephone networks; see for example [Ber91]. However, overload control should only be active rarely; otherwise, the system has not been properly dimensioned.

Other ways of handling these problems is to use *service-level agreements* (SLA). Typical operational performance characteristics that are agreed upon in an SLA include charging criteria, minimum delay, throughput, and availability. The focus within this section is on SLAs located in gateways between a mobile network and an application server with emphasis on the application layer. An SLA may contain hard or soft time constraints. A hard time constraint for some class of tasks requires that they all should be finished before a deadline. A soft time constraint may demand that the mean time to complete a service should be smaller than some limit or that a certain fraction of the tasks should be ready within a limit. An SLA is usually implemented by a token bucket, call gapping, or a similar algorithm, which both can reduce the rate of requests and also shape the traffic.

Next, results on the following problems for service architectures are summarized:

- How to design an overload control mechanism?
- How to dimension servers and gateways?
- How to set the parameters, for example, for a token bucket such that an SLA is not violated?

What methods can be used to solve problems like this? Simulation is of course always possible to use. However, it suffers from the usual disadvantages of long execution times and sometimes results that are difficult to interpret. Network Calculus [Bou04] can be used to study hard time constraints. However, when having soft time constraints, Network Calculus is too pessimistic,

which leads to overdimensioning and/or setting the wrong parameters in the SLAs. In these cases, queuing theory may be used.

A number of papers discuss the problems sketched above. In [And00, And04], a Parlay X application server is modeled, its performance is investigated, and two overload control mechanisms are proposed. The overload control mechanisms support performance agreements of different kinds. Requests may have different priorities, and guaranteed acceptance ratios are considered. Simulations and testbed implementations are used to evaluate the proposed mechanisms. In [And05a, And05b], the impact that different constraints placed on the incoming traffic have on performance and guarantees is studied. A scenario with hard time constraints is analyzed by Network Calculus. Simulations are used to study soft time constraints. In [And06], Network Calculus and queuing theory are used to dimension gateways. Guidelines on when to use which methods are presented, and examples of dimensioning are provided. A fuller description of the results summarized in this section can be found in [TD(06)002].

3.2.2 Packet-Level Models

Wireless channels are characterized by dynamic time-varying behavior often leading to incorrect reception of channel symbols. These errors may propagate to higher layers of the protocol stack resulting in the loss of protocol data units at those layers. In this environment, even if a connection is admitted at call level, packet-level performance may be unacceptable. In this section, three contributions describing packet-level performance models are presented. The first two contributions thus propose performance models for wireless channels with *automatic repeat request* (ARQ) and *forward error correction* (FEC). The first one focuses on a general channel, whereas the second one introduces a model for the IP packet delay in a UMTS network. The third contribution reviews analytic models for queuing systems with bursty arrival processes.

3.2.2.1 Modeling of the Frame Transmission Process Over Wireless Channels

The performance of servicing systems in communications networks may vary in response to changes in first- and second-order arrival statistics. Emerged methods of measurement-based traffic modeling allowed recognizing statistical characteristics of the traffic affecting its service performance [Li97a, Li97b, Haj98]. According to Li and Hwang [Li97a], the major impact on performance parameters of the service process is produced by the histogram of relative frequencies of the arrival process and the structure of the *autocorrelation function* (ACF). Hayek and He [Haj98] highlighted the importance of marginal distributions of the number of arrivals showing that the queuing response may significantly vary for inputs with the same mean and ACF. It was also shown

[Li97b] that an accurate approximation of empirical data can be achieved when both marginal distribution and ACF of the model match their empirical counterparts well.

Wireless channels are characterized by even more complicated environment, where both arrival and service processes are stochastic in nature. The straight way to model the frame transmission process over a dedicated *constant bit rate* (CBR) wireless channel is to use a $G_A/G_S/1/K$ queuing system, where G_A is the frame arrival process, G_S is the service process of the wireless channel, and K is the capacity of the system. The service process is defined as the times required for successfully transmitting successive frames over the wireless channel. Characteristics of this process are determined by the frame error process and error concealment schemes of the data-link layer.

It is known that both frame interarrival time and transmission time of a frame – from the first transmission until the successful reception – are generally not independent. These properties make the analysis of a $G_A/G_S/1/K$ queuing system a quite complex task even when arrival and service processes can be accurately modeled by Markov processes. The theoretical background of queuing systems with (auto) correlated arrival and service processes is not well studied. Analyzing these systems is computationally more expensive compared with queuing systems with renewal service processes. It usually involves embedded Markov chains of high dimensions. From this point of view, such a performance model does not provide significant improvements over other approaches.

In [TD(05)008, Mol05], Moltchanov considered a class of preemptive-repeat priority systems with two Markovian arrival processes. Both processes are allowed to have arbitrary autocorrelation structures of Markovian type. Assume that the first arrival process represents the frame arrival process from the traffic source. For providing an adequate representation of the unreliable transmission medium, the assumption is made that the second arrival process is a one-to-one mapping of the frame error process. That is, every time an error occurs, an arrival from this arrival process takes place. In what follows, we refer to this process as "error arrival process." An illustration of the mapping is shown in Fig. 3.6, where the time evolution of a data-link layer wireless channel model and the corresponding artificial arrival process is shown. In the figure, gray rectangles denote incorrect frame receptions and arrows indicate arrivals. According to this mapping, probabilistic properties of the stochastic model remain unchanged. Making this process to be the high-priority one, and allowing its arrivals to interrupt the ongoing service of low-priority frames, ensures that when an arrival occurs from this process, it immediately seizes the server, while the ongoing service is interrupted. A frame whose service is interrupted remains in the system and allocates the server again after the service completion of the high-priority arrival. The service time provided until the point of interruption is completely lost. It is interpreted as an incorrect reception of the frame from the traffic source, and the priority discipline is referred to as preemptive-repeat.

Fig. 3.6 Mapping between channel model and artificial (error) arrival model (gray rectangles denote incorrect frame receptions and arrows indicate arrivals)

To emulate the behavior of *Stop and Wait-ARQ* (SW-ARQ) protocols, the assumptions are made that, first, an infinite number of retransmission attempts is possible and, second, that the feedback channel is completely reliable (perfect). Indeed, feedback acknowledgments are usually small in size and well protected by FEC. Furthermore, the feedback is assumed to arrive instantaneously. These assumptions were tested and used in many studies and found to be appropriate for (relatively) high-speed wireless channels [Zor97]. Because the wireless channel model was extended to the data-link layer, FEC capabilities are explicitly taken into account. Note that the described model is also suitable to represent "ideal" *Selective Repeat-ARQ* (SR-ARQ) scheme [Com84]. In SR-ARQ, frames are continuously transmitted and only incorrectly received frames are selectively requested. According to "ideal" operation of SR-ARQ, *round-trip times* (RTT) are assumed to be zero. In this case, SR-ARQ and SW-ARQ schemes become identical and can be represented using the proposed model.

Analysis of queuing systems with priority discipline is still a challenging task. Among others, preemptive-repeat is probably the most complicated priority discipline. However, a number of assumptions can be introduced to simplify the queuing model. In what follows, the model is limited to the discrete-time environment and requires each arrival from any arrival process to have a service time of one slot in duration. According to such a system, arrivals occur just before the end of slots. Because there can be at most one arrival from the arrival process representing the frame error process of the wireless channel, these arrivals do not wait for service, enter the service in the beginning of the next slot, and, if observed in the system, are being served. For providing an adequate representation of the erroneous nature of the wireless channel, the model has to ensure that all these arrivals are accommodated by the system. Following these assumptions, preemptive-repeat priority discipline is no longer required. Because all arrivals occur simultaneously in batches, it is sufficient for such a system to have non-preemptive priority discipline. The resulting system takes the form of a $G_A + G_E/D/1/K$ non-preemptive queue, where G_A is the frame arrival process, G_E is the artificial error arrival process, and K is the capacity of the system.

The proposed framework allows investigating the influence of first- and second-order arrival and channel statistics on performance response of wireless channels analytically. For example, in [Molxx], the proposed model was used to demonstrate that the mean number of lost packets in a slot, and mean frame

delay may significantly vary for different values of lag-1 autocorrelation coefficient of the frame error and arrivals processes.

3.2.2.2 Modeling the IP Packet Delay in UMTS Networks

Whereas the last section proposed a model for the frame transmission time resulting from a general wireless channel, the focus is now on the delay of an IP packet in a UMTS network where a SR-ARQ mechanism is applied on the *Radio Link Control* (RLC) layer. Usually, cellular mobile networks provide sequence integrity and deliver IP packets in-order to higher layers. As a consequence, the loss of a MAC frame will delay the delivery of all subsequent correctly received frames until the lost MAC frame has been retransmitted successfully. This additional delay is usually referred to as reordering delay or resequencing delay.

Resequencing delays have extensively been studied in the past. In [Ros89], Rosberg and Shacham derive the distribution of the resequencing delay and the buffer occupancy in an SR-ARQ system. Their underlying system is a slotted system, where each slot is protected by SR-ARQ, and one arriving packet fits into a single slot. A similar assumption was made by Konheim in [Kon80]. In [Ros03], Rossi and Zorzi present an accurate heuristic approach to evaluate the delay of packets in UMTS networks. The authors consider both SR-ARQ and in-order delivery and use their analysis to determine the optimal number of retransmission attempts on the RLC layer.

This section gives a summary of a similar model for the IP packet delay that was developed in [Nec05, TD(05)014]. First, a model is provided that covers the ARQ mechanism in UMTS, and then the *complementary cumulative distribution function* (CCDF) of the IP packet delay is analytically derived. The final result can be used to implement a simple model for the IP packet delay in a network level simulator, which allows the investigation of higher layer protocols and services with respect to their performance in mobile environments without the need to implement a detailed model of the Radio Access Network.

In UMTS, an IP packet is segmented into b RLC block sets, which are then transmitted within one TTI. Each RLC block set is assumed to be lost with equal and independent probability P_L. If a loss is detected, the RLC block set is retransmitted, where the retransmission may be lost again. Accordingly, the number of necessary transmission attempts follows a geometric distribution. Note that in UMTS DCHs, retransmissions take place between UE and RNC and the Node-B is oblivious to the correctness of the transmissions.

Let us first consider the reordering delay for an isolated IP packet. Assume that the time T_{RTT} between transmission and retransmission is larger than the time of b TTIs required for transmitting all RLC block sets of an IP packet. Then, the delay of the IP packet is determined by the RLC block set with most retransmissions. Assuming independent losses of RLC block sets, the probability for observing a reordering delay of $n \cdot T_{RTT}$ for an isolated IP packet corresponds with the probability that at least one RLC block set experiences n

retransmissions and no RLC block set experiences more. Let $N_{RLC,i} \sim Geom(P_L)$ be a random variable for the number of retransmissions of RLC block set i of an IP packet. Then, the delay of an IP packet is equal to

$$X_{IP} = \max_i \{N_{RLC,i}\} \cdot T_{RTT}. \tag{3.2}$$

The CCDF $\bar{F}_{IP}(t)$ of X_{IP} is a stair function that can be approximated by the exponential function

$$\bar{F}_{IP}(t) \approx e^{\ln P_L / T_{RTT}} = \tilde{F}_{IP}(t). \tag{3.3}$$

Note that the exponent is always negative because $P_L < 1$. A detailed derivation of this result can be found in [Nec05, TD(05)014]. Figure 3.7 compares the accurate and approximate CCDF for loss probabilities of 15% and 30%. The approximation shows a good match to the original CCDF, which could even be improved by time-shifting the approximation to the right. In general, we can say that the approximation may even better resemble the behavior of a real UTRAN system, as the hard steps of the original CCDF are avoided.

Considering a sequence of IP packets and not only an isolated IP packet, the reordering delay of packets at the receiver becomes important. Let $T_i \sim X_{IP}$ be

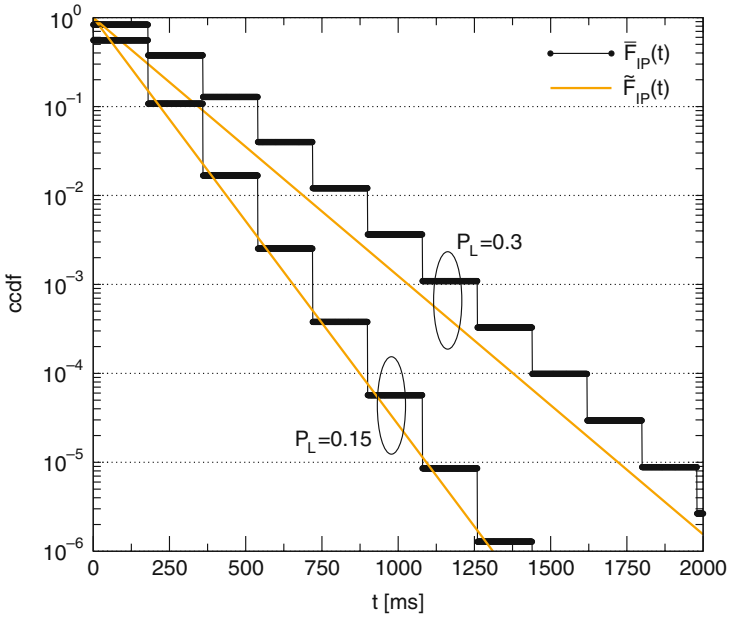

Fig. 3.7 CCDF of the delay of an isolated IP packet

the delay of the i-th IP packet and t_i its arrival time. The i-th IP packet is delivered when both all its own RLC blocks are successfully received and IP packet $i-1$ is already delivered to the higher layer. Accordingly, the reordering delay X_i for an in-sequence packet can be written recursively as

$$X_i = \max\{X_{IP}, X_{i-1} - (t_n - t_{n-1})\}. \tag{3.4}$$

Applying the exponential approximation for the CCDF of the delay of an isolated IP packet, we obtain

$$\tilde{F}(t) = 1 - \prod_{i=0}^{\infty} \left(1 - e^{\ln P_L / T_{RTT} \cdot (t + i \cdot b \cdot T_{TTI})}\right). \tag{3.5}$$

In order to derive delay statistics on IP layer including correlation properties, an abstract queuing model for the UMTS data link is constructed. An IP packet is first stored in the radio network's input buffer. The UMTS data link reads the packets from the buffer at the effective line speed. Subsequently, a read packet is delayed by the line speed transmission time and additional processing, propagation, and fixed network delay. Finally, the IP packets experience the reordering delay at the receiver. This behavior can directly be mapped to an abstract queuing model as shown in Fig. 3.8.

A traffic source generates IP packets, which are stored in a bounded FIFO queue. Subsequently, a single server delays the IP packets according to the effective line speed of the radio link. The subsequent infinite server accounts for processing and propagation delays and for the delay introduced by the core network and the Internet. The final infinite server accounts for the reordering delay introduced by the ARQ mechanism. Its service time follows a general distribution, which can be approximated by the described model. Note that this model can easily be implemented in a network-level simulator. For further

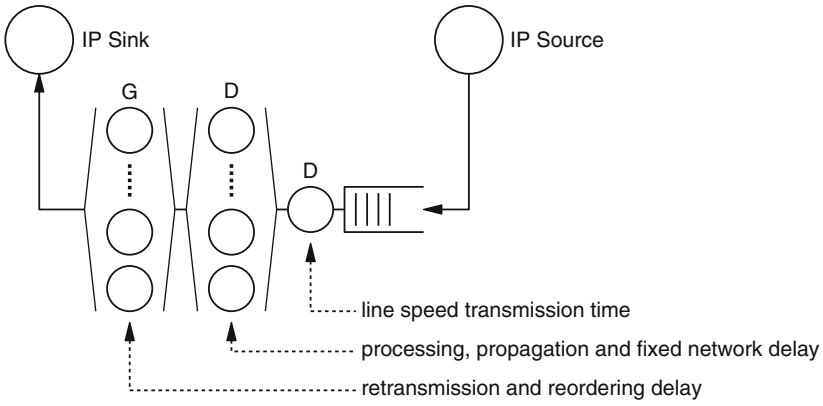

Fig. 3.8 Queuing model for the UMTS radio link

information, please refer to [Nec05, TD(05)014], which also contains a detailed study and validation of the application to transport protocol investigations at the example of TCP simulations.

3.2.2.3 Enhanced Queuing Models for Wireless Networks

The future wireless access network must be able to cope with the higher throughput and more elastic traffic demand required for exploiting multimedia services, the scarcity and deployment difficulty, the heterogeneity of different radio air interface, and the high cost of network deployment and operation. A solid understanding of traffic processes is a prerequisite for designing proper wireless networks. The development and enhancement of general queuing models as described in this section allows the designer of wireless networks to better understand the impact of traffic characteristics like burstiness on the network performance.

Many studies on traffic measurements from a variety of packet-switching networks, such as Ethernet, Internet, and ATM, have shown considerable difference between actual network traffic and assumptions in traditional theoretical traffic models. The basic characteristic of traffic found in modern telecommunications networks is burstiness, whereas traditional theoretical traffic models consider only Markovian traffic. That is why there are now many studies that generalize the queuing systems by state-dependent arrival and service rates.

This section considers a generalized input Poisson stream that can be peaked, regular or smooth, and is defined by a state-dependent arrival rate. The stationary probabilities of a full accessibility queuing system M(g)/M/S (by Kendal notation) with a generalized Poisson input stream M(g), exponential service time M, and number of the servers and sources S are described by a generalized Erlang distribution. The generalized arrival and service flow with nonlinear state dependence is used to study the new models for loss and delay queuing systems [Mir05].

The authors of [TD(05)034] analyze a M(g)/M/n/k/S queue with a generalized Poisson arrival process, exponential service time, multiple servers, limited waiting positions, and finite number of customers. The idea is based on the analytic continuation of the Poisson distribution and the classic Erlang's delay system M/M/n. The techniques are applied on the basis of birth and death process and state-dependent arrival rates. The influence of the peaked factor on the congestion probability, the mean system time, and the waiting time distribution are studied. It is shown that the variance of the input stream significantly changes the characteristics of the delay systems.

The model presented in [Mir06] belongs to the class of queuing systems with feedback. It is a M(g)/D/1/k/S queue with generalized Poisson arrival process, constant service time, single server, limited waiting positions, and finite number of customers. This model with quasi-random input stream and constant service time is a non-Markov process (renewal process). An algorithm for the

calculation of the state probabilities, the time congestion probability, the average delay, and the waiting time distributions are presented. It is shown that the influence of the peakedness over the performance measures is significant.

[Mir07, TD(07)007] deals with a full accessibility loss system and a single server delay system with a Poisson arrival process and state-dependent exponentially distributed service time. The generalized service flow with nonlinear state dependence mean service time is considered. The idea is based on the analytical continuation of the Binomial distribution and the classic M/M/n/0 and M/M/1/k system. These techniques are applied on the basis of birth and death process and state-dependent service rates.

Next, let us focus on the system M/M(g)/n/0 and M/M(g)/1/k with a generalized departure process: M(g). The output intensity depends nonlinearly on the system state with a defined parameter: "peaked factor, p." State probabilities of the system can be obtained by using the general solution of the birth and death processes. The influence of the peaked factor on the state probability distribution, the congestion probability, and the mean system time are studied. It is shown that the state-dependent service rates significantly change the characteristics of the queuing systems.

The advantages of simplicity and uniformity in representing both peaked and smooth behavior make these queuing models attractive for the analysis and synthesis of wireless QoS networks. These generalized models can be used to analyze multiplexing, message storage, traffic regulator, and communication network performance.

3.3 Performance Evaluation Based on Simulations and Measurements

The methodology for performance evaluation of mobile and wireless communication systems can be categorized into analytic methods, abstract simulations, detailed protocol simulations, and measurements in testbeds or real-life networks. Whereas Section 3.1 described analytic and abstract simulation models, this section addresses detailed protocol simulators and measurements. Consequently, the focus of this section is more on the obtained performance results than on model development and description. Regarding protocol simulators, we distinguish system-level simulation and link-level simulation. Section 3.2.1 describes the results of two simulation studies on *Enhanced UMTS* (E-UMTS) networks. The simulator [SEA, Cab06a] captures the dynamics of the end-to-end behavior within an entire UMTS network including the support of enhanced functionalities. The multiservice traffic simulator focuses on modeling the teletraffic behavior in a set of neighboring cells in the presence of mobility [Jua06, Jua07].

Section 3.2.2 presents results from a link-level simulation. Different triggers for switching modulation and coding are investigated for the operation of single-carrier IEEE 802.16 over High Altitude Platforms (HAPs).

Section 3.2.3 presents results from real-network measurements. The capacity of an HSDPA cell is investigated by connecting multiple HSDPA devices to a single macro-cell and executing different test scenarios like Web navigation or file transfers in parallel.

Section 3.2.4 finally describes an Simple Network Management Protocol (SNMP)-based measurement system for monitoring the capabilities for generating and capturing traffic of different network interface cards.

3.3.1 Protocol Simulator for Large-Scale E-UMTS Networks

E-UMTS is mainly seen as the introduction of the HSDPA in 3GPP Release 5. However, the enhancements go far beyond HSDPA and include also the "all IP" architecture, several link layer enhancements, and techniques for QoS support in an "all IP" UMTS network. While minimizing network operation costs, the goal of the all-IP network is to enable broadband wireless access operators to move from being mere connectivity providers to being full-service providers, offering Internet connectivity, voice services, and broadcast/multicast and next-generation broadband services to end users, all from a single network.

One of the key properties of WCDMA systems as already shortly discussed in Section 3.2.1.1 is that the system is interference limited, which leads to the effect of cell breathing: highly loaded cells have a small coverage area, whereas lowly loaded cells have a larger coverage area. Accordingly, coverage and capacity planning are closely related and must be considered simultaneously in the dimensioning process. In general, radio network planning includes the dimensioning of detailed capacity and coverage planning, as well as network optimization. Dimensioning as a first step in the planning process [Lem04, Lai06] estimates an approximate number of base station sites, base stations and their configurations, but also other network elements, based on the operator's requirements and the radio propagation in the area. The dimensioning must fulfill certain requirements for coverage, capacity, and QoS. The input to the dimensioning process is hence the initial requirements for coverage, capacity, and QoS, as well as the area type and the radio propagation models.

This section addresses the main issues for achieving a simulation environment that enables coverage and capacity planning for an E-UMTS mobile network and presents relevant results obtained for different environments. For evaluating the performance of E-UMTS by a detailed system-level simulator, specific scenarios and identify characterization parameters are defined. The scenarios are in the form of subproblems, dealing with different environments and parameter sets [TD(05)015].

One of the key problems when developing a simulation-based planning process is to select an appropriate traffic model as in principle a well-designed protocol simulator allows the planner to simulate an arbitrary mixture of applications and their mapping on service classes. The key lies in finding the right compromise between a most realistic application mix and the ability to reduce the set of applications such that the effects of single applications are still discernible. In general, when modeling applications, there are many parameters to be considered [Fer05, TD(05)006]. These parameters include (1) service parameters like delivery requirements (real-time or non–real-time traffic), intrinsic time dependency (time-based or non–time-based traffic), unidirectional or bidirectional, unicast or multicast; (2) traffic parameters like the generation process, the distribution of the duration, the average connection duration, or the transmission data rate; (3) communication parameters like the burstiness, the *bit error rate* (BER), the communication protocol, and (4) session and activity parameters like the busy hour call attempt and inter-arrival time, the arrival distribution, the average active/inactive time and its distribution, the duration and its distribution.

3.3.1.1 Coverage and Capacity Planning Methodology

This section shortly describes the process of performing a simulation-based radio network planning study [TD(05)015]. An overview of the process is shown in Fig. 3.9. Coverage and capacity planning strongly depends on the selected scenario (i.e., parameters such as site selection, antenna-specific parameters, propagation, and traffic and mobility models). The first step is to select the

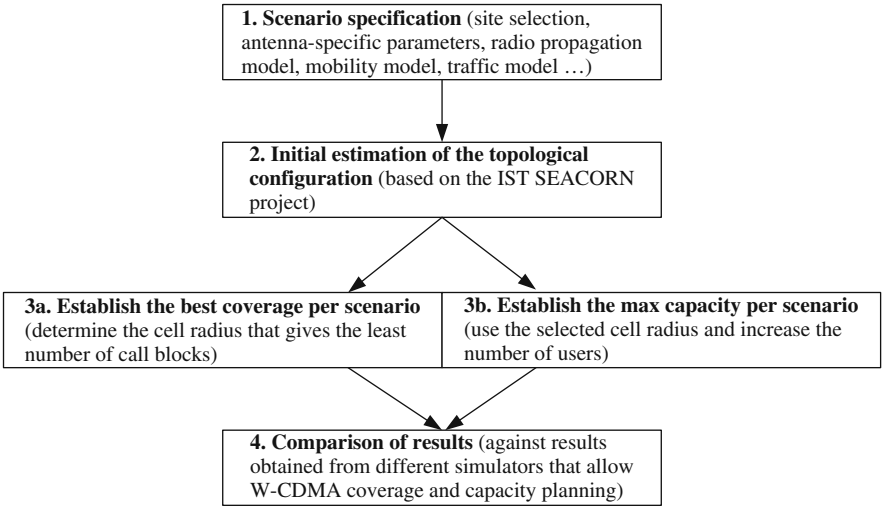

Fig. 3.9 E-UMTS coverage and capacity planning methodology

parameters characterizing the specific scenario. The planning problem is mainly specified by the propagation model and the traffic model; therefore, they need to be carefully defined for each scenario, so as to "closely" represent reality.

Next, an iteration roughly estimating a reasonable configuration of Node-Bs is done. Two sets of simulations are run for each scenario. For the first set of simulations, the values of the cell radii are varied while keeping the rest of the scenario parameters constant. The best cell radius, hence, the best cell coverage, is found for the lowest value of the number of blocked calls in a simulation run. Once the best cell radius is determined for each scenario, a set of simulations with varying number of users per environment is run. The aim is to determine the maximum capacity that can be supported in this specific scenario.

Finally, for validation purposes, a comparison of this coverage and capacity results is performed with the outputs from other simulators (available in the literature).

In the following, some results on the optimal cell density in certain environments are shown that were obtained by using a system-level protocol simulator [SEA] according to the planning methodology described above. Under consideration are the office, the urban, and the *Business City Center* (BCC) scenarios as presented in Chapter 6 [TD(05)006, Fer05]. By taking into account a worst-case situation between the grade of service constraints like blocking probability P_b, handover failure probability P_{hf}, delay, and delay variation, the most suitable values for the throughput, *thr*, are found for different cell radii R [Cab06b, Cab06c, TD(05)051]. Figure 3.10 shows the throughput *thr* versus the radius. Fitting the curve yields that the throughput can be approximated as a function

$$thr(R) = 37.145 \cdot R^{-0.7225} \tag{3.6}$$

of the cell radius. The parametric values correspond with a scenario in which all services are taken into account simultaneously and the blocking probability P_b is the only constraint. In contrast, for the detailed services approach (i.e., when

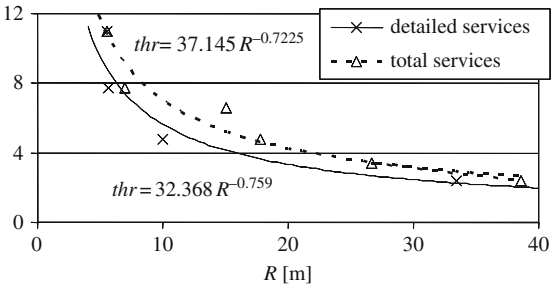

Fig. 3.10 Total supported throughput in office environments

discriminating the individual results for the different services classes and not the global ones), the supported throughput is

$$thr(R) = 32.368 \cdot R^{-0.759}. \tag{3.7}$$

The lowest values obtained for the throughput in the latter approach are more accurate because the blocking probability for the wideband class – a non–real-time application – is not considered. As a consequence, the acceptable radius slightly decreases.

The results suggest that a smaller cell radius leads to a higher throughput and accordingly has a potential for higher revenue. On the other hand, a smaller cell radius is achieved by a higher Node-B density associated with higher investment costs.

Relying on the detailed services approach, results for the most profitable cell radius are obtained via an optimization procedure based on economic aspects as specified in Chapter 6. A higher number of pico-cells (with a smaller radius, around 30 to 32 m) can be installed in the future when costs for deploying and maintaining the network decrease, as such allowing the support of higher system capacity and reducing prices.

Regarding the urban scenario with the detailed services approach, mathematical models were obtained for the supported fraction of active users and for the supported throughput, as a function of the cell radius, while guaranteeing a given *grade of service* (GoS). Two different configurations are considered: base stations with one and three amplifiers. By using a curve fit approach [TD(06)045, Cab06a], the curve for the supported throughput can be approximated as:

- One amplifier: $thr(R) = 1/\left(-0.2262 + 0.0079 \cdot R^{0.65905}\right)$
- Three amplifiers: $thr(R) = 1/\left(-6.425e-2 + 1.6696e-4 \cdot R^{1.1039}\right)$

Figure 3.11 shows the gain in throughput and cell density, respectively, when using three amplifiers instead of one amplifier.

Regarding the BCC scenario, by joining together the blocking and the handover failure probabilities constraints into a new quality parameter, a different type of analysis was performed. Instead of using the lowest value for the throughput that satisfies both blocking and handover failure restrictions, the

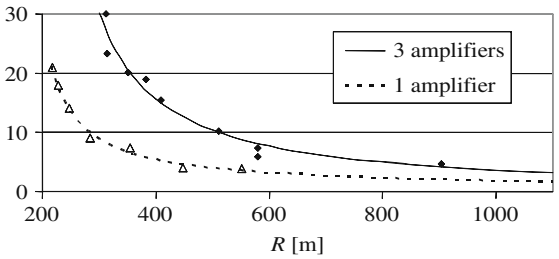

Fig. 3.11 Total supported throughput in the urban scenario

concept of quality parameter, QP, was introduced. The quality parameter joins together, in a unique QoS parameter, the number of blocked calls (*nb_blocked_calls*), the number handover failures (*nb_interrupted_calls*), and the total number of calls (*total_nb_call*) as follows [Vel07a, TD(07)046]:

$$QP = \frac{nb\_blocked\_call + 10 \cdot nb\_interrupted\_call}{total\_nb\_call}. \tag{3.8}$$

The idea of the QP is to have a single target value for designing the network. The factor of 10 expresses the higher user dissatisfaction from call dropping than from call blocking. The threshold assumed for QP is 1%. A lower grade of service corresponds with a higher quality of service. As the supported throughput varies within the covered area, it is presented per km^2. The supported throughput in Mbit/s/km^2 was found to be

$$thr(R) = 58587604.876 \cdot 10^{-0.039R-6} + 2618775.763 \cdot 10^{-0.0047R-6}. \tag{3.9}$$

It is a function decreasing with the cell radius, and varies from ~6.0 Mbit/s/km^2 down to ~400 kbit/s/km^2. This decreasing behavior may be due to the fact that as the users are getting further away from the Base Station (BS), the BS has to increase the power in order to serve the same user, causing more interference and the reduction of the BS resources (power). In Chapter 6, besides the economic analysis, results for cellular planning optimization based on cost/revenue issues can be found.

3.3.1.2 Teletraffic Simulation for Mobile Communication Systems Beyond 3G

In Beyond 3G systems like E-UMTS, the number of available resources is not fixed but depends on power constraints and services mixtures. Consequently, the planning process has to be flexible and needs to be automated as far as possible. The process of obtaining the maximum sustained traffic for a given number of resources in a multiservice scenario can be supported via modeling approaches. A model accounting for the multiservice nature of traffic and including the impact of mobility can be very useful. A simulator was produced to extract conclusions about blocking and handover failure probabilities in a multiservice traffic context [Jua07]. Various multiservice models were built with the most relevant activity/inactivity characteristics of this technology in different scenarios. The simulator was developed with AweSim, a general-purpose simulation system for network discrete-event and continuous simulation approaches [Jua06, Jua07, TD(06)017].

By considering the deployment scenario characteristics, the teletraffic parameters from the *Vehicular* (VEH) scenario [TD(05)006, Fer05] and the burstiness of traffic, simulations were performed for different cases, from single-service to multiservice situations, and from absence to presence of mobility [TD(06)017, Jua06]. Values for the usage were extracted from Table 6.1 in Section 6.2.3 of

Chapter 6, and the session activity parameters for the active and inactive states are extracted from Table 6.2.

The simulator is also very useful for extracting conclusions about the validation of the Bernoulli-Poisson-Pascal model for the computation of the *on*/*off* blocking probability $P_{b,ON/OFF}$. This probability corresponds with the ratio of the number of calls rejected at the beginning of *on* periods, in the process of allocating a channel, and the total number of *on* bursts generated during a session.

Results for bursty voice traffic are shown in Fig. 3.12 comparing theoretical and simulation results for $P_{b,ON/OFF}$ for different loads ρ and the handover rate γ as parameter. The theoretical and the experimental values of $P_{b,ON/OFF}$ are close to each other. The right-hand graphic of Fig. 3.12 shows a special example for $\rho = 0.15$ Erl, and there is an almost perfect concordance between theoretical and simulation values for $\gamma = 1$ (i.e., when the average sojourn time in cells is equal to the average holding time). The curves for the blocking probability P_b and the handover failure probability P_{hf} follow a similar behavior but P_{hf} takes lower values. A mixture of voice and video traffic was also chosen for the multiservice case. Detailed results and a throughput discussion can be found in [Jua07].

3.3.2 Adaptive Modulation and Coding for HAP Communications

The scarcity of radio spectrum necessitates its opportunistic usage, with the physical layer transmission parameters being dynamically adjusted according to the current channel quality. Achieving this, diverse approaches can be employed. This research work is concerned with the evaluation of a particular AMC scheme for the operation of the IEEE 802.16 standard [802.16d] over *High Altitude Platforms* (HAPs). In particular, the link is assumed to be based

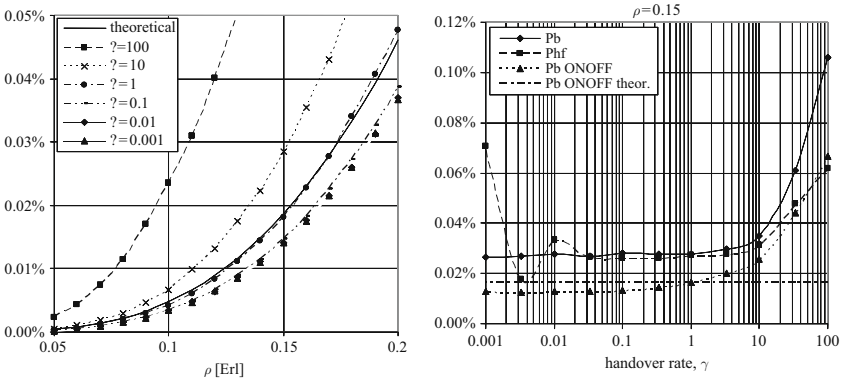

Fig. 3.12 Theoretical and simulation results for $P_{b,ON/OFF}$

on the IEEE 802.16 standard's single carrier air interface for operation above 10 GHz. In the proposed AMC procedures, the major interest was on investigating parameters acquired from the channel decoder, thus making transitions between different transmission schemes more reliable. Aiming to adequately take into account the impact of used arithmetic and the influence of quantization noise due to AD/DA conversions, the selected procedures were implemented on a digital signal processing board and tested on a HAP propagation channel model. The latter has been, due to lack of previously available statistical HAP channel model or propagation measurement campaigns for HAP-terrestrial radio links, developed on a basis of the land-mobile satellite propagation channel model [Lut91]. It is composed of a ray-tracing-approach–based finite state machine, modeling very slow channel variation due to transitions among areas with different environmental conditions (i.e., LoS, shadowed, and blocked channel state), and a stage modeling slow and fast channel variations with each area's probability density function describing statistical channel properties. The main differences with respect to the LMS propagation channel model taken into account when modeling HAP propagation conditions refer to significantly shorter distance between the transmitter and the receiver, and different rate of elevation angle and its unpredictable nature [Jav05].

The IEEE 802.16 standard specifies the common medium access control layer and several physical layers of broadband wireless access system. Considering the aim of this study being the implementation and investigation of AMC procedures, the focus lies on physical layer specifications only, where all relevant functionalities reside. Given that the propagation channel from base station to various subscriber stations is different, the transmission format of the physical layer is framed in such a way that it supports adaptive profiling in which transmission parameters, that is, modulation (QPSK, 16-QAM, or 64-QAM) and coding, can be adjusted individually for each subscriber stations on a frame-by-frame basis. The supported frame durations are 0.5 ms, 1 ms, and 2 ms. The frame starts with a preamble that is used for synchronization and equalization. The latter is based on a constant amplitude zero autocorrelation (CAZAC) sequence, composed of 16 or 32 QPSK modulated symbols.

The concept of AMC procedures is to maximize the spectral efficiency at a given target block error rate. This is achieved by adapting the coding type and modulation mode at the transmitter based on the receiver's feedback on the estimated channel quality. In other words, in higher signal-to-noise ratio (E_s/N_0) environment, a coding-modulation scheme with higher spectral efficiency but lower power efficiency is used and vice versa. Various criteria can be used to select the most appropriate coding type and modulation mode, whereas in our AMC scheme, switching is controlled with a careful combination of two parameters, that is, the estimated E_s/N_0 and the Reed-Solomon (RS) decoder state. The estimated E_s/N_0 is within the receiver obtained by calculating E_s/N_0 ratio for each sample of the CAZAC sequence and consequently averaging over the entire sequence. The RS decoder state is the parameter representing the number of bytes RS decoder has been able to correct in the previous frame. Both

parameters are for each frame being forwarded to the transmitter, where the *AMC switch* according to the parameters' average values performs the switching requests. In order to define values at which switches between transmission schemes should occur, the RS(255,239) coded QPSK, 16-QAM, and 64-QAM modulation schemes were tested in the Additive White Gaussian Noise (AWGN) channel.

Based on these initial results, three switching scenarios [Smo07, TD(07)019] were defined for the targeted BER defined as 10^{-3}. These are the *without RS*, *only RS,* and *with RS* scenario. In the first, transitions between transmission schemes are performed by only using the estimated E_s/N_0 values; in the second, where possible, using only the RS decoder state value; and in the third by combining both values. In a given scenario, the parameters values for "up" and "down" switching do not differ, hence this may lead to switching oscillations between neighboring transmission schemes. In order to avoid such oscillations, a hysteresis is introduced by taking the switching decision based on the average value of parameters over five frames. The operations of each switching scenario in an AWGN channel are in terms of spectral efficiency depicted in Fig. 3.13. The switching scenarios have a similar efficiency, which means that the information on the number of bytes corrected by the RS decoder in previous frames can be in some cases used equivalently to the estimated E_s/N_0 value at the receiver.

Finally, in order to test the switching scenarios in a realistic propagation environment and find out their average spectral efficiencies, the simulations have been repeated in a HAP propagation channel model. The simulation results for the switching scenario, combining both the estimated E_s/N_0 value and the RS decoder state, are depicted in Fig. 3.14. The upper graph depicts the

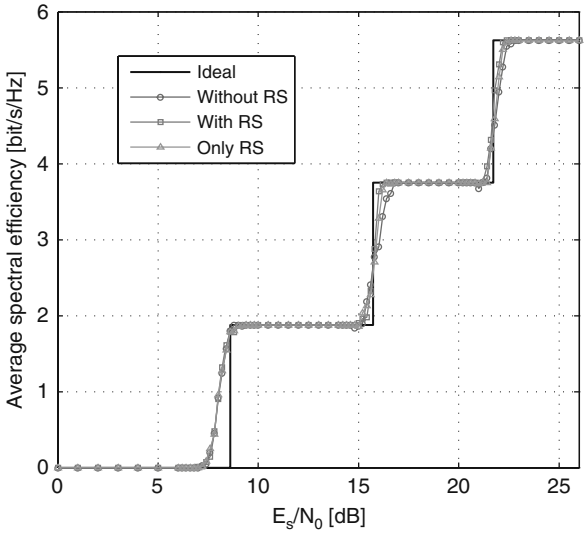

Fig. 3.13 Average spectral efficiency for different switching scenarios in AWGN channel

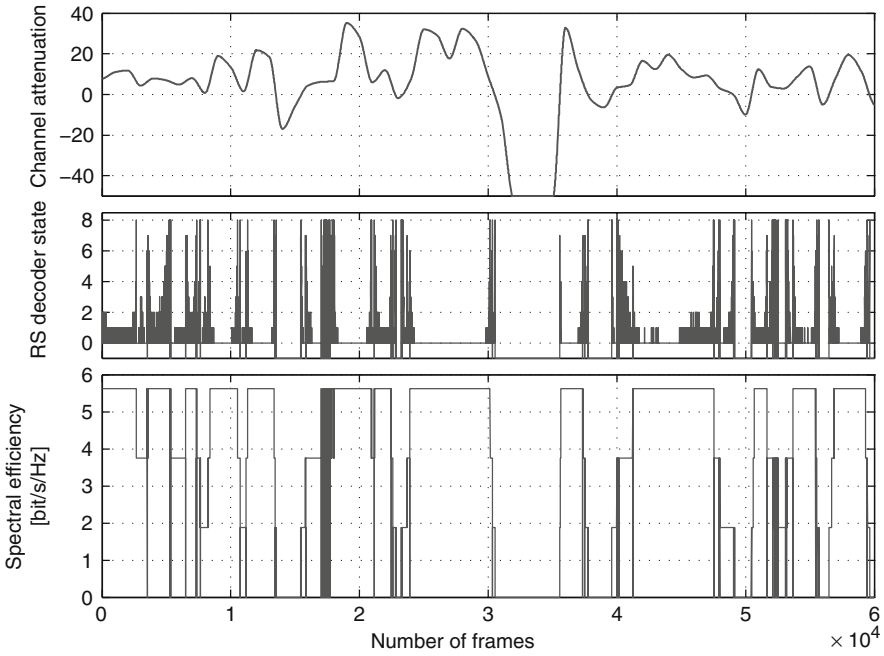

Fig. 3.14 FEC performance and spectral efficiency in HAP channel (copyright © 2007 IEEE [Smo07])

channel attenuation over 60,000 frames, the middle graph shows the RS decoder state in a given frame in terms of the number of corrected bytes (with the value –1 denoting that RS was no longer able to restore the original data), and the bottom graph gives the current spectral efficiency. Comparing the average spectral efficiencies of all three scenarios on the same section of railway track leads to the conclusion that switching based only on the RS decoder state information (for "down" switching), that is, the *only RS* scenario, provides similar performance to the *without RS* scenario, where only the value of estimated E_s/N_0 is observed when deciding for a switch. Moreover, the *with RS* scenario combining information on RS decoder state and estimated E_s/N_0 further improves the performance in terms of average spectral efficiency.

3.3.3 HSDPA Performance Based on Measurements

The performance of HSDPA has been largely investigated in the past years. Most of the studies, however, rely on analytical models or simulation techniques, in general following a more or less theoretical approach; see the discussion in Section 3.2.1.1. As the number of HSDPA networks in operation grows and users start using them, there is a lack of knowledge about the real performance

provided by this technology. Some recent papers present results based on measurements in a laboratory [Hol06a], in scenarios that clearly differ from the real conditions found in a live HSDPA network. In this respect, it is worth mentioning a few studies based on measurements of commercial HSDPA networks [Der06, Jur07]. These studies, however, focus on measurements related to one HSDPA user, without taking into account the influence of other simultaneous HSDPA users sharing the capacity of the cell. Although this aspect can be neglected in early HSDPA network deployments, as the number of users increases it should definitely be taken into account.

Precisely one of the main contributions of this work is the realization of measurements in a scenario with multiple HSDPA users accessing the same cell. As the traffic load in many UMTS/HSDPA commercial networks is rather low, HSDPA traffic was generated by several students participating in the measurement experiments. The results motivated the investigation of the impact of TCP (Transport Control Protocol) configuration parameters on the observed performance, concluding the convenience of employing large TCP receive window sizes. Further details can be found in [TD(07)033].

The measurement scenario located in a teaching laboratory at the Universidad Politécnica de Madrid is within the range of an HSDPA/UMTS macro-cell covering the university campus. A total of 28 students, subdivided on two shifts, participated in the measurements campaign. The experiments were carried out from 1100 to 1400 on work days (i.e., during the network's busy hours). Each student had a desktop computer with a Category 6 (3.6 Mbit/s) HSDPA device. The students performed several basic experiments including Web navigation sessions, Web-based on-line speed tests, and file downloads.

During the first experiment, students conducted a 5-minute Web navigation session. Figure 3.15 shows the probability density function (PDF) and the complementary cumulative distribution function (CDF) for the downlink peak rate of the experiments. The average download peak rate was 870 kbit/s, with 85% of the users obtaining a peak rate above 550 kbit/s. These bit rates are at application level, which in part explains why the figures are below the physical bit-rate of the employed HSDPA devices (3.6 Mbit/s). In addition to protocol overheads, we should also consider the non-optimum indoor

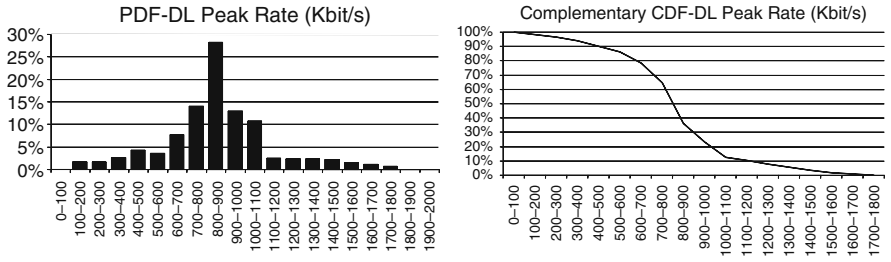

Fig. 3.15 Results for HSDPA Web navigation experiments

propagation conditions at the laboratory, the non-HSDPA traffic load in the cell (the experiments were run at the busy hour), and, of course, the relatively high number of HSDPA users in the cell (a dozen). Taking into account these considerations, we can conclude that the results are quite satisfactory.

In the next experiment setup, users downloaded a number of files from a FTP (File Transfer Protocol) server. Three different file sizes were considered: 100 Kbyte, 1 Mbyte, and 10 Mbytes. For each file size, the experiment was repeated four times. For comparison purposes, the same experiments were performed previously with a single HSDPA user in the cell. The results are summarized in Fig. 3.16. For the single-user case (left-hand graphic), the average download throughput was between 500 kbit/s and 950 kbit/s, while the maximum download throughputs ranged from 675 kbit/s to 1100 kbit/s. It is worth observing that the results are considerably better for large file sizes. In the multiuser scenario (right-hand graphic), the average download throughput was between 450 kbit/s and 640 kbit/s, while the maximum throughputs ranged from 850 kbit/s to 1100 kbit/s. When interpreting these results, one should observe that the experiments were not synchronized (i.e., the users decided freely on the time they started the file downloads without taking into account how many of them were simultaneously connected to the FTP server). While in principle this approach does not allow for accurately interpreting the effect of the HSDPA capacity sharing, it has the advantage of being more in line with the traffic observable in real networks, where the user behaviors are not scheduled.

In order to evaluate the impact of the TCP configuration on the HSDPA performance, the FTP experiments were repeated for the single-user case varying the TCP receive window size and turning on and off the SACK (selective acknowledgment) option. The results are summarized in Fig. 3.17. The results show that – except for the smallest file – the TCP receive window size has a significant impact on the download throughput. In general, increasing the

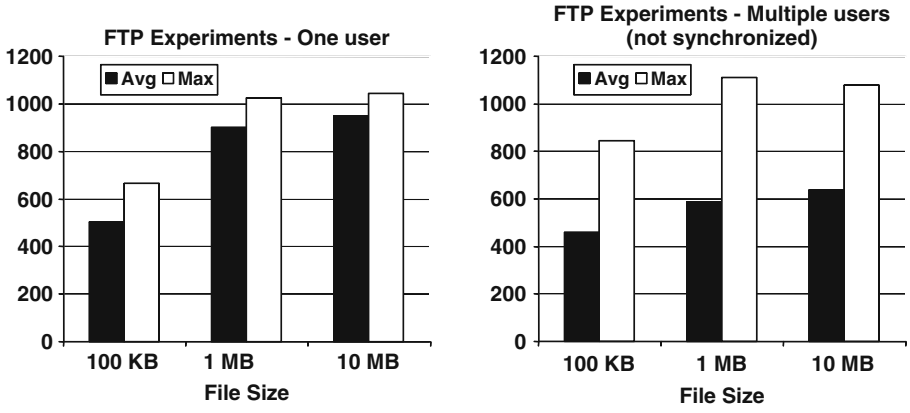

Fig. 3.16 Results for HSDPA file transfer experiments

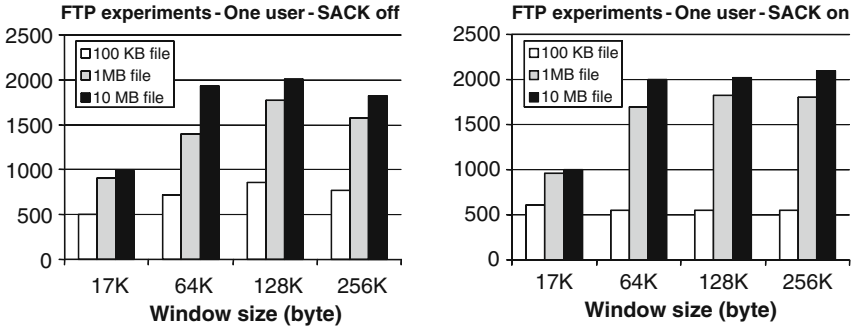

Fig. 3.17 Impact of TCP parameters in the results of FTP experiments

window size leads to higher bit rates. However, there is a maximum window size that, if exceeded, makes it necessary to turn the SACK option on in order to avoid throughput degradation. For small file sizes, using large TCP windows and SACK does not seem to provide any performance improvement. The explanation is that for short file sizes, the TCP connection setup hand-shake procedure and the slow start mechanism do not allow exploitation of the high capacity available in the HSDPA link. This conclusion is quite interesting as it leads us to reconsider the results of the Web navigation experiments. Recent studies report a typical Web page size of around 130 Kbytes [Lev06], which is close to the smallest file size considered in our experiments. Therefore, we can conclude that for conventional Web navigation, the moderate size of Web pages themselves does not permit full exploitation of the high bit rates provided by HSDPA. For further results and interpretation, please refer to [TD(07)033].

In this section, results on the performance of TCP applications over HSDPA based on measurements on a commercial network were presented. One of our main contributions is the realization of measurements in a scenario with multiple HSDPA users simultaneously accessing the same cell. Despite the high variability of the results, the experiments with Web traffic show that the user-perceived quality is very satisfactory and similar to the one achievable with an ADSL line of 1 Mbit/s.

Results for file transfer experiments, far from exhaustive, reveal the capacity sharing effect on the HSDPA downlink channel. In addition, we observe that small file sizes exhibit a download throughput lower than expected, as the transfer finishes before the maximum bit rate can be reached. Considering typical Web page sizes ($\sim$130 Kbytes), we conclude that conventional Web navigation cannot fully exploit the HSDPA capacity.

Our final set of experiments focused on evaluating the effect of TCP receive window size and SACK option. The results indicate that for traffic volumes above 1 Mbyte, large receive window sizes (128 Kbytes or more) and SACK lead to higher download throughputs (up to 100% increase in some experiments).

3.3.4 QoS Monitoring Tools

This section summarizes the results of [Bik06, TD(06)050] presenting a measurement system for monitoring the capabilities of different network interface cards – with respect to both traffic generation and capturing. Such an evaluation is useful for assessing the quality of tools analyzing captured traffic and measuring QoS performance. The presented communication of the management information takes place between an administration console and a set of distributed SNMP-based software measurement agents for GNU/Linux platforms. The software features a graphical user interface and a group of services that handle the management information. The services are used to communicate with the operating system's socket interface and to perform SNMP encapsulation and decoding. A measurement session manager has the intelligence of interpreting the measurement results. A queuing service solves the issue of asynchronous communication by implementing a set of eight message-waiting queues. Four priority levels exist, complemented by a round-robin servicing policy to ensure that management messages are handled in the following order: notifications, control messages, results requests, and results replies. The advantages of the proposed measurement solution versus the existing tools give the possibility of managing many test scenarios through the control of a large set of agents. No user attendance is required during the experiments, sessions are customizable, and numeric or plotted results are available both during and after the measurement is completed [Bik06].

The functionality of the management infrastructure is divided into several operational units called services. All components (except Session Manager and Service Control Manager) are found on the manager and the agent platforms; the overall structure as illustrated in Fig. 3.18. is symmetrical.

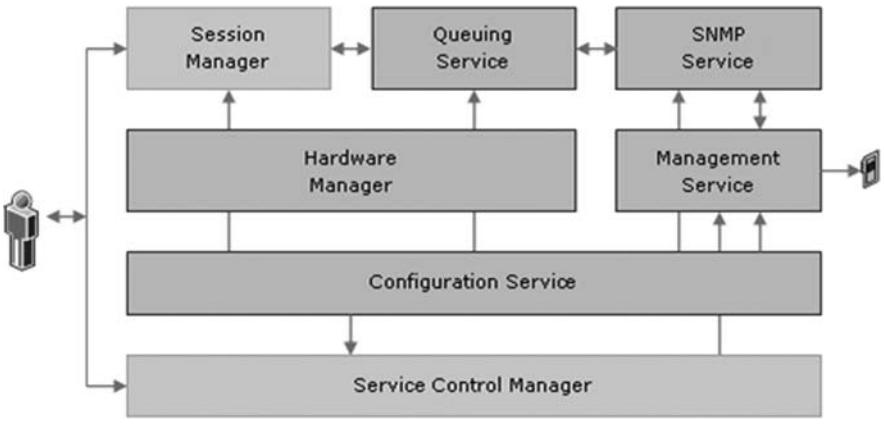

Fig. 3.18 Management infrastructure architecture (copyright © 2006 SOFTCOM [Bik06])

Table 3.2 Sessions (copyright © 2006 SOFTCOM [Bik06])

SessionType	Agents Used	Description
Generation	1	It uses one agent to generate the network traffic.
Analysis	1	It uses one agent to analyze the network traffic.
Generation and analysis	2	It uses two agents, one for the generation and one for the analysis. The session is flow-based, meaning that only the traffic generated by the first agent will be analyzed by the second one.

Therefore, it does not matter what functionality (management/measurement) the application has. The Management Service handles networking functions (i.e., transmission and reception of management packets for any selected local interface). Outbound, the destination address and port are given by the Session Manager, which knows which agents are used within the test. The Management Service performs bidirectional multiplexing and de-multiplexing of the messages to be added or retrieved from the message queue. It also implements security functions by filtering the IP addresses of inbound messages, according to a user-defined list. The task of the Queuing Service is to ensure that multiple simultaneous incoming or outgoing management messages can be processed. In addition, this service establishes priorities on the messages placed in the queue and handles retransmissions. It also ensures that duplicate messages arriving within the duplicate discarding interval are eliminated. Queuing Service performs the recycling (i.e., the messages waiting more than the permitted time are removed from the queue). The Session Manager is the highest-level software routine of the infrastructure, implemented at the management console only and performing functions related to measurement. The user interaction means setting up a test by creating sessions as summarized in Table 3.2, session groups and scheduled tasks [Bik06]. From the management's point of view, the measurement tasks scheduled by the user are translated into appropriate SNMP messages, to be sent to the agents. When the first reply is received, a session is created. The results for each task are stored in order to make them available for later inspection. The Service Control Manager is implemented only at the management console and it handles all services operation. It also performs service recovery in the situation of a service failure; several recovery actions being possible to define.

3.4 User-Perceived Quality of Service

As of today, adopters of QoS support for real-time services over the Internet infrastructure can back on the achievements of roughly two decades of research as well as segmental deployment. Yet, however, a QoS featuring Internet on a global scale still seems distant. This matter recently has induced the scientific

community to revise the foundations of QoS as a subject in itself, including its definition. As a result, Internet QoS, formerly a purely technical term expressing physically measurable quantities like information loss or delay, commonly called *Intrinsic QoS* (IQ), has obtained a second definition expressing highly subjective human perception of quality, called *Subjective QoS* (SQ). It seems that, at last, the Internet research community became aware of what has been well known for the Public Switched Telephone Network (PSTN) for decades; humans' cumulative subjective quality rating is the ultimate measure.

This section first gives an insight to the difference of IQ and SQ by investigating the impact of lost packets in particular at the cell edge. Then, it provides an overview on methods for estimating video quality and shortly introduces two new methods developed within the framework of the COST 290 Action. After focusing on the assessment of user-perceived quality, two examples are presented how to use these measurements for resource control. Finally, a simulation study compares the impact of different voice coding schemes with respect to experience voice quality and network resource requirements.

3.4.1 User-Perceived Quality, Assessment, and Critical Impact

Although an increasing number of scientists endorse SQ, this awareness still has not penetrated the Internet Engineering Task Force (IETF), the principal Internet standardization body. But there is an obvious reason for that. Engineers deem IQ favorable, because it is founded on well-understood theories, directly measurable and displayable using highly subjective opinion charts, which are the original SQ assessment tool for expressing the perception of test subjects participating in a controlled experiment.

Nevertheless, albeit the sole method for capturing all features of SQ assessment will always remain surveying humans, scientists have conceived a hybrid method, the so-called Objective or Instrumental QoS (OQ). The rationale of this method is to combine both approaches by measuring physical performance parameters and subsequently map them to SQ on the basis of functions determined by extensive human surveying.

Current mobile telecommunication networks support high enough QoS in the majority of cases. Conventional statistical methods reveal that average network quality is quite tolerable. Despite this, even well-developed networks fail to deliver a satisfactory QoS in particular conditions at some locations [Kaj04]. There is a problem with statistics, because calls of poor quality tend to occur at particular locations. Users being in some "bad" locations suffer from poor quality frequently, much more frequently than does an average user. Such locations of poor quality often are at the cell edges.

The edge of a cell is the terrain at marginal distance from the base station. Some peculiarities of communications at the cell edge can be pointed out as follows: higher transmit power (critical limit of power may be reached $P = P_{\max}$), lower

received power, enlarged inter-cell interference, lower C/I (carrier-to-interference ratio), higher probability of handover, increased packet loss rate.

As an example, QoS peculiarities at cell edge are investigated on the basis of GSM (Global System for Mobile Communications) networks. With the currently deployed networks, 3G networks often do not provide complete coverage but are complemented by GSM networks in rural areas so quite frequently handovers from 3G cells to GSM cells occur. A method for collecting lost speech frame traces of individual users in GSM systems is proposed in [Kaj06, TD(05)050, TD(06)030, TD(07)030].

The analysis of frame loss traces, experimentally collected for users at the cell edge in a measurement campaign, shows that it is possible to model flows of lost packets using a two-state Markov chain. Transition probabilities of the chain depend on C/I values. A model constructed in such a way is capable of reproducing series of lost packets with sufficient precision [Kaj06]. Table 3.3 shows transition probabilities for different C/I ranges. Here p_{00} is the probability that the next packet will also be correctly received under the condition that the current one is correct. If the current packet is erroneous, the probability for losing the next one as well is p_{11}.

The impact of lost packets on speech quality is very specific, because losses make a speech signal dissimilar to the original signal. The loss of a packet means that some information is inevitably lost, and receiving subsequent packets correctly is not sufficient for restoring the lost information. A lot of research has been carried out on the effects of packet losses on speech quality under different transmission conditions (see, e.g., [Cla01, Sun01]). Currently, the most prominent method for predicting the voice quality as an average is the PESQ algorithm [P.862]. The impact of a series of lost packets on voice quality is shown in Fig. 3.19 presenting estimated rates of quality degradation values for different packet loss rates (PLR). The results are obtained by simulations using two arbitrarily chosen 2 s length sentences denoted (a) and (b) in Fig. 3.19. The quality degradation values are marked as dQ_{PESQ} . As we can see, the dQ_{PESQ} rates are distinct for all loss models and both sentences. Even 1% of lost packets may cause high-quality degradation (dQ_{PESQ} up to 1.6), though the rate of this occurrence is not large. But when 5% to 7% of packets are lost, the quality degradation dQ_{PESQ} may be up to 2.0 to 2.6 and the rate of such occurrence increases, too.

From these examples, it can be seen that the conventional average is not the best choice for estimating the perceived conversational speech quality in mobile networks. An average does not reflect the real speech quality perceived by a particular user. For this reason, in mobile networks, perceived speech quality shall be measured explicitly for each individual user.

Table 3.3 Transition probabilities for different C/I

C/I, dB	3...5	6...10	11...15	16...
p_{00}	0.72294	0.91488	0.9932	0.99992
p_{11}	0.74443	0.54515	0.43119	0

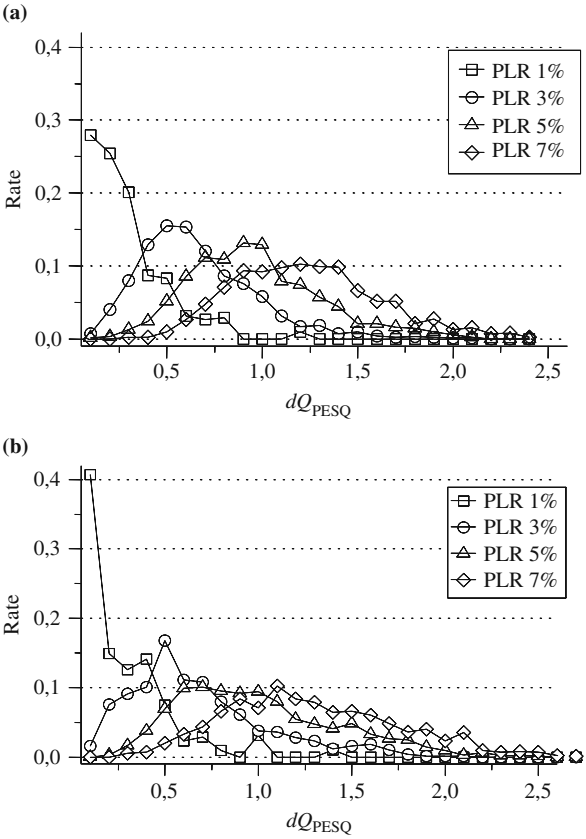

Fig. 3.19 Examples for distributions of dQ_{PESQ} occurrence rates

3.4.2 Video Quality Estimation for Mobile H.264/AVC Video Streaming

For the provisioning of video streaming services, it is essential to provide a required level of customer satisfaction, given by the perceived video stream quality. It is therefore important to choose the compression parameters, as well as the network settings, so that they maximize the end-user quality. Because of video compression improvement of the newest video coding standard H.264/AVC, video streaming for low-bit and frame rates is allowed while preserving its perceptual quality. This is especially suitable for video applications in 3G wireless networks.

Mobile video streaming is characterized by low resolution and low bit rate. The commonly used resolutions are *Quarter Common Intermediate Format* (QCIF; 176 × 144 pixels) for cell phones, and *Common Intermediate Format* (CIF; 352 × 288 pixels) and *Standard Interchange Format* (SIF or QVGA; 320 × 240 pixels) for data-cards and *palmtops* (PDA). The mandatory codec for

UMTS streaming applications is H.263 but 3GPP Release 6 [26.234] already supports a baseline profile of the new H.264/AVC codec [H.264]. The appropriate encoder settings for UMTS streaming services differ for various streaming content and streaming application settings (resolution, frame and bit rate) as is demonstrated in [Nem04, Kou05, Rie05, Joh06].

3.4.2.1 Experimental MOS Score for UMTS Video Streaming

Mobile video streaming scenarios are specified by the environment of usage, streamed content, and the screen size of the mobile terminal. Therefore, the mobile scenario is strictly different in comparison with classic TV broadcasting services or broadband IP-TV services. Furthermore, most of the mobile content is on demand. The most frequently provided mobile streaming contents are news, soccer, cartoons, panorama for weather forecast, traffic, and music clips. An extensive survey shows systematic differences between *Mean Opinion Score* (MOS) results obtained by testing on UMTS terminals and PC screens [Nem04] in a measurement campaign. According to these experiences, the tests performed on UMTS mobile terminals also do not follow ITU-T Recommendation [P.910]. In order to emulate real conditions of the UMTS service, only in this single point, all the sequences were displayed on a PDA. The test method was Absolute Category Rating (ACR) as it better imitates the real-world streaming scenario. Thus, the subjects did not have the original sequence as a reference, resulting in a higher variance. The sequences were presented in arbitrary order and the test environment followed the ITU recommendation. People evaluated the video quality after each sequence using a five-grade MOS scale (1, bad; 5, excellent) in a prepared form. The obtained MOS data as displayed in Fig. 3.20 was scanned for unreliable and inconsistent results.

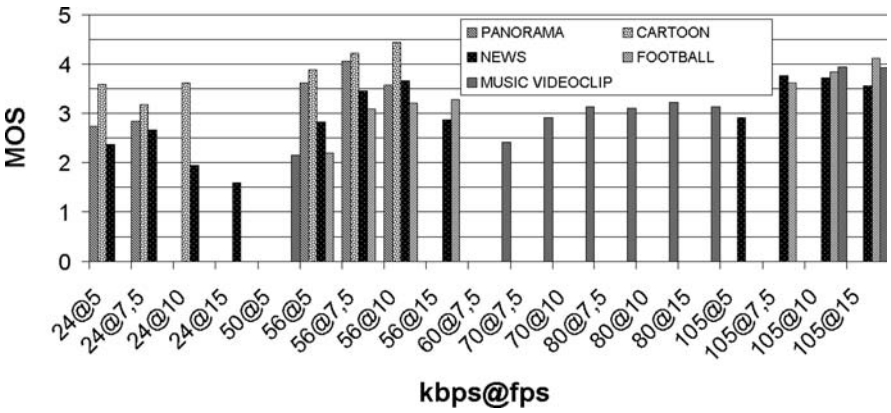

Fig. 3.20 MOS for all tested content types (copyright © EURASIP [Nem04])

3.4.2.2 User-Level Video Quality Estimation

In the past years, several objective metrics for perceptual video quality estimation were proposed. The proposed metrics can be subdivided into two main groups: human-vision-model–based video metrics [Rix99, Ong03, Win03, Win05] and metrics based only on objective video parameters [ANSI, Mar02, Pin04, Kus05]. The complexity of these methods is quite high and they are mostly based on spatial features, although temporal features better reflect perceptual quality, especially for low-rate videos. Most of these metrics were designed for broadband broadcasting video services and do not consider mobile video streaming scenarios.

In [TD(05)037, TD(06)047], a method is proposed for estimating the video quality of mobile video streaming at the user-level (perceptual quality of service) for any possible codec settings in 3G networks and for any content type. The objective is to find measures that do not need the original (noncompressed) sequence for the quality estimation, because this reduces the complexity and at the same time broadens the possibilities of the quality prediction deployment. Hence, the target is to find an objective measure of video quality simple enough to be calculated in real time at the receiver side. New reference-free approaches for quality estimation based on motion characteristics are presented. Both estimation methods use temporal segmentation [Dim05] before quality estimation. Furthermore, both methods are based on content/character-sensitive parameters. The main difference between them is the estimation process alone.

The first approach [Rie07a] introduces a quality metric based on five content adaptive parameters, allowing for content-dependent video quality estimation. The model reflects direct relation of objective parameters to MOS.

The second approach [Rie07b, TD(06)047] estimates video quality in two steps. First, the content classification with character-sensitive parameters is carried out. The content classification is based on the statistical and resolution-independent features of motion vectors (MV) and color distribution within one shot. Finally, based on the content class, frame rate, and bit rate, the video quality is estimated.

The proposals for quality estimation are trade-offs between applicability, processing demands, and prediction accuracy. The first proposal is more complex but allows us to divide content classification and quality estimation as illustrated in Fig. 3.21. The suitable solution is to perform the content class classification at the streaming server and stream content information with video. Finally, the quality estimation is performed at the user equipment. This allows us to estimate the quality at the receiver with extremely low complexity. The next approach allows for a full-reference free estimation at the sender and receiver sides. Currently, this proposal is more suitable for streaming servers due to limitations in processing power at the user devices. In comparison with the well-known ANSI metric [ANSI], our proposals are less complex and more accurate, although the ANSI metric was not designed for video streaming services.

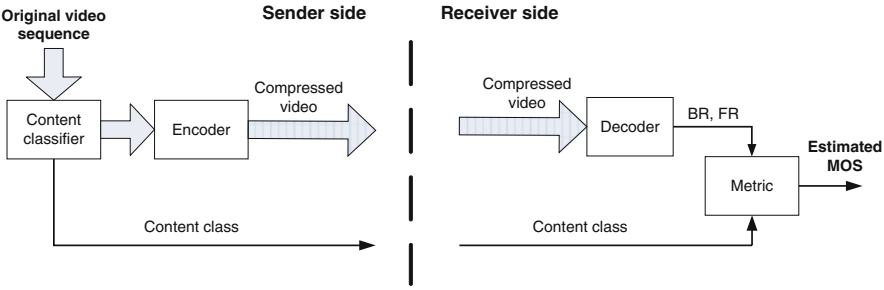

Fig. 3.21 Content-based video quality estimator design

3.4.3 User-Perceived-Quality–Based Resource Control

Being aware of the significance of SQ as such, the question is whether it can be actively controlled by mechanisms as commonly practiced in the case of IQ. The principal rationale is to monitor OQ levels and feed this information back to actively control elements at certain network locations. For a better illustration of this principle, the sequel of this section elaborates this idea in greater detail by two standard QoS control examples: adaptive video transmission and admission control.

3.4.3.1 Adaptive Video Transmission Over the Wireless Internet

In the past, Internet traffic was dominated by applications that required reliable data delivery and used TCP connections (e.g., FTP, HTTP, etc.), whereas streaming media demands low and predictable latency and often, high data rates. The Internet, however, is characterized by large variations in available network bandwidth and host processing power, resulting in potentially high variance in latency. The problem is worsened when considering the rising demand for wireless video streaming, which is driven by the rapidly growing user base equipped with high-capacity mobile devices like phones, PDAs, and laptops. Also, today's Internet does not seem to provide adequate QoS guarantees capable of fulfilling strict video transmission requirements.

Bearing this in mind, QoS adaptation schemes are required to address the problem. An effective adaptation scheme can be based on the observation that several applications can operate with acceptable performance when the provided QoS fluctuates within certain limits. By taking advantage of this fact, a system can be designed to adjust the QoS the network offers to application requirements in order to increase network capacity when possible, by allowing more concurrent user sessions, and ensure acceptable QoS support. Thus, scalable and adaptive techniques should be developed in order to cope with the different constraints, capabilities, and requirements of various networks and end users' applications.

The prime criterion for the video quality is SQ, which is considered to be a reliable method that can be measured through SQ assessment methods. In particular, the perceived measure of the quality of a video is done through the human "grading" of streams, which helps collect and utilize the general user view (MOS). However, subjective assessment is an expensive and time-consuming procedure, impracticable for real-time quality monitoring. Thus, OQ methods are required, as, for example, the Peak Signal-to-Noise Ratio (PSNR), which is solely based on physical measurement but produces results comparable with those of subjective tests. On the other hand, these metrics cannot characterize fully the response and the end satisfaction of the viewer. In order to correlate these two methods, we study the relationship between the MOS and the PSNR, which is presented in [Vas06].

Current Internet transport-layer protocols do not provide any QoS guarantees for video streaming. UDP offers no congestion control mechanism and therefore is unaware of the network condition and can be unfair toward other competing traffic. TCP uses several mechanisms to handle congestion, but the introduced packet delay results in video quality degradation. Several approaches and mechanisms have been proposed for Internet video streaming. A *TCP-friendly equation-based congestion control* (TFRC) [RFC3448] proposed for unicast continuous streaming applications is not considered robust to wireless losses. Most TCP-friendly streaming control protocols including [Cen98, Yan04] try to reduce congestion and provide smoother transmission rate with controlled and predictable delay. On the other hand, video rate adaptation mechanisms like [Rej99, Jac98] have been proposed in order to adapt the video content to available network bandwidth taking into account end users' overflow conditions and network state. Moreover, the existing fuzzy-based video rate control techniques [Saw98, Tsa98] focus on buffer occupancy, without considering the network state.

This section, summarizing [Ant07a, Ant07b, TD(07)031], is focused on Content Adaptation Techniques (CATs) working together with Network Adaptation Techniques (NATs). CATs deal with adaptation of content to the desirable transmission rate using primarily layered video approaches, whereas NATs deal with the end-to-end adaptation of video application needs to the network parameters, using algorithms that take into account the state and/or load of the network. The goal of [Ant07a, Ant07b, TD(07)031] was to develop a fuzzy-based rate control mechanism to support high-quality, smooth, efficient, and friendly video streaming in the wireless Internet. In particular, the approach combines an adaptive feedback mechanism with a fuzzy decision algorithm for video streaming over the Internet. The assumption is made that each video stream is encoded in multiple layers stored at the sender side. The feedback mechanism combines receiver's critical information on the perceived quality, as well as measurements obtained by the core network, in order to evaluate the available bandwidth of the network path. The estimated available network bandwidth is then fed into the decision algorithm, which decides in a fuzzy manner the optimal number of layers that should be sent.

The approach is evaluated under error-free and error-prone environments, as well as under various cross-traffic patterns. The results indicate that the algorithm can finely adapt the video stream bit rate to the available bandwidth and maintains responsiveness to various traffic patterns like CBR, FTP, and Web-like cross-traffic. It was discovered that the system achieves robustness and loss tolerance that does not deteriorate the OQ (and the SQ) the way the video packet loss does. Also, OQ remains acceptable even in the presence of FTP and Web cross-traffic. It was demonstrated that the system is able to scale up offering graceful performance degradation, and at the same time the available bandwidth is fairly shared between active users who receive almost the same quality in terms of PSNR.

User-Perceived-QoS–Based Admission Control

Among many others, one of the functions intentionally left unspecified by the IEEE 802.16 standard body is Admission Control (AC) as neither of both standards, IEEE 802.16d [802.16d] for fixed broadband wireless access (BWA) nor 802.16e [802.16e], the amendment for mobile scenarios, specify any AC mechanisms. Notwithstanding, IEEE 802.16d defines a comprehensive Quality of Service (QoS) model that itself depends on AC. Given this void, Bohnert et al. present in [Boh08] "an Admission Control (AC) algorithm for the specific case of pre-provisioned IEEE 802.16d links for VoIP aggregates."

The presented algorithm approaches the AC problem from a different perspective and is based on a cross-layer design. As metric for quality of VoIP services, it applies SQ assessment based on speech quality. It is evaluated at application layer by OQ assessment, which in turn builds on statistics from the packet loss process captured on MAC layer. Finally, QoS control in form of AC is applied on MAC and IP layer.

The *de facto* OQ assessment method is the E-Model [G.107]. Its original application domain is network planning, and one of the questions answered in [Boh08] was if it lends itself for online resource management, in particular if applied to VoIP aggregates. Therefore, the latest definition of the E-Model was deployed, including extensions to capture in-stationary packet loss processes and the delayed perception of quality level changes by humans, based on the findings presented in [Raa06]. In brief, the *aggregate* packet loss process is being monitored online, and changes in the packet loss distribution are detected, based on a slightly modified approach as presented in [Cla01]. At the transition between two different periods of loss process characteristics, the loss ratio is calculated and the related impairment factor is computed by a functional determined by extensive SQ assessment experiments. This results in a series of so-called loss impairment factors. These impairment factors are averaged taking into account the delayed perception feature of human memorial capabilities and behaviors with respect to quality changes. Finally, at admission request, the average impairment factor is used as the respective E-Model factor together with some standard parameters and an upper-bound for delay impairment. This

combination allows computing the R-Score expressing human service quality perception, so-called *integral quality based on averaging* [Raa06]. This allows the definition of an AC algorithm similar to [Boh07a] on whose basic policy new calls are admitted if the R-Score is above a predefined quality level, else rejected.

In order to determine the applicability of this AC algorithm, it was subjected to extensive simulative scrutiny. The first feature under investigation was accuracy as this is a fundamental problem largely unsolved for measurement-based AC algorithms [Boh07b]. The evaluation criterion in such an evaluation is how closely an AC algorithm approaches the configured QoS target, in this case the contracted R-Score (R-Target) expressing speech quality of VoIP conversations. Hence, for a first simulation set, the R-Target was set to 85, and as shown in Fig. 3.22, this target was achieved for most of the time. Skipping the transient phase, the average estimated R-Score for the remaining time was 86.82, the standard deviation was 3.89, and the minimum and maximum R-Score were 59.97 and 98.89. Additionally, the longest continuous period the R-Score was continuously below the R-Target was *t-max* = 39.87 s. This simulation has been repeated for different R-Targets between 80 and 90 that correspond with the MOS "Satisfied." The results indicate a consistent performance albeit the AC appears a bit too conservative for low R-Target values.

As *t-max* appears large at first sight, let us investigate the CDF of the time spans *t* during which the instantaneous R-Score continuously stays below the R-Target. For the whole range of R values, the average time spent below R-Target is approximately 10 s. The probability that the time span is larger than 20 s is around 20%. This clearly qualifies the large value for *t-max*.

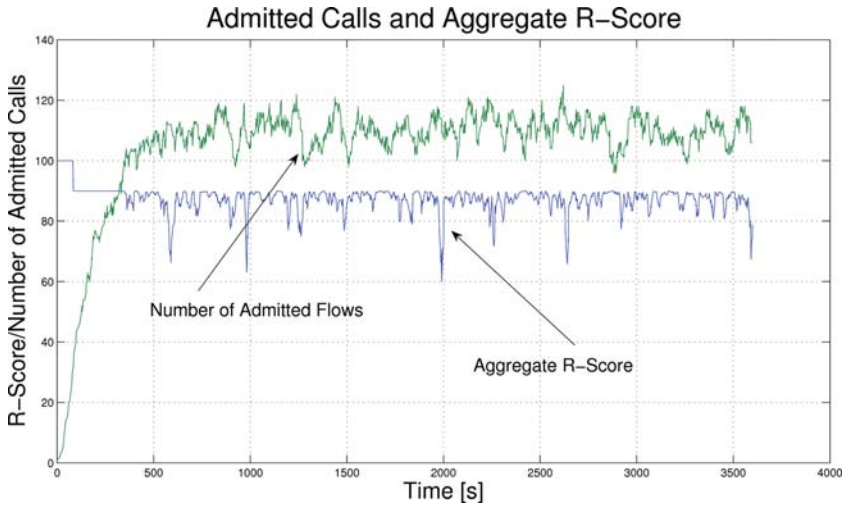

Fig. 3.22 Number of admitted calls and R-Target for a VoIP aggregate over time (copyright © 2008 IEEE)

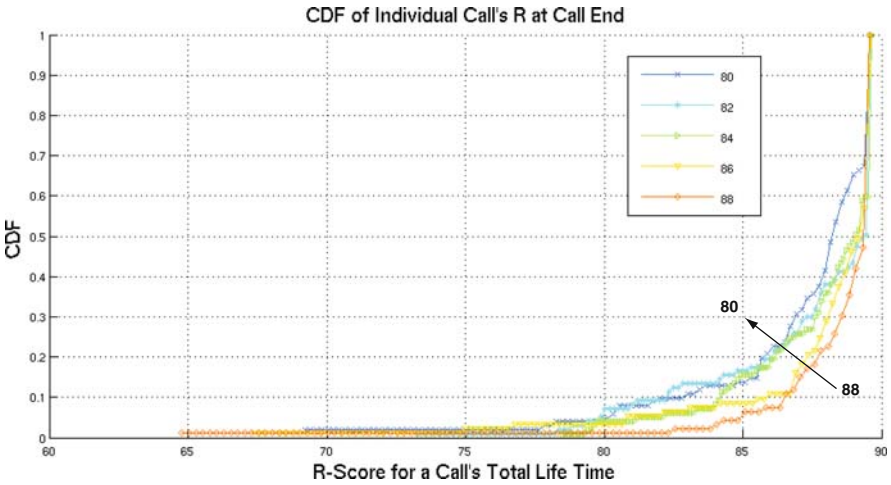

Fig. 3.23 CDF of single call quality for a set of randomly recorded calls for all simulations. For each simulation, less than 5% of calls fall below R = 80 (copyright © 2008 IEEE).

A second evaluation set was carried out in order to evaluate if the central assumption, that a slightly modified E-Model parameter computation allows application of the E-Model on aggregate scale, holds. In order to do so, 100 randomly selected, consecutively admitted flows were recorded, and the R-Score for each individual call has been computed using the original E-Model parameter computation. Hence, SQ for each individual flow's total lifetime was assessed, and Fig. 3.23 plots the CDF of these calls' R-Scores.

The figure shows that for each R-Target, maximally around 5% of calls are rated below R = 80, which is the lower threshold for "Satisfied" on the MOS scale. Taking the first simulation, depicted in Fig. 3.22, as an example, it means that approximately 6 of 110 concurrently admitted flows on average would be affected by lower QoS than contracted. However, some of them fall in the range R = [70, 80], which maps to MOS "Some User Dissatisfied," meaning that some of these may still rate "Satisfied."

Finally, the conclusions drawn from Fig. 3.23, with respect to configuration and QoS versus resource utilization trade-off, is that if an operator wants to ensure that less than 2% of calls fall below R = 80 (MOS: Satisfied), the R-Target should be set to 88. Obviously, the higher the QoS demands, the lesser the network utilization. An operator can weight user satisfaction and resource utilization. It appears that for this setup, an R-Target set to 84 achieves the best trade-off as there are around 5% of calls rated below MOS "Satisfied" while roughly half of them are still in the range of MOS "Some Users Dissatisfied."

3.4.4 Evaluation of the Coding Scheme Impact on IP-QoS Network Utilization and Voice Quality

This section summarizing [TD(07)009] aims at revealing criteria for decisions concerning the speech coding scheme used in voice over IP (VoIP) applications over QoS-aware networks. Such criteria should be based on evaluations of the coding schemes' impact on network utilization and voice quality impairments. Speech quality impairment evaluations are based on the ITU-T E-Model [G.107, G.108] for objective evaluations of quality degradations, as an alternative to the subjective MOS. The performance evaluations concerned six speech coding schemes specified by ITU-T and European Telecommunications Standards Institute (ETSI) (GSM).

The simulation framework used in the evaluations is IT Guru tool from OPNET [OPNET]. Based on simulation results, different aspects of the coding schemes' impact on network load and voice quality were analyzed and certain ways for exploiting these aspects were found so that the network load and voice quality can benefit. The network model as shown in Fig. 3.24 consists of two routers (*Router_1* and *Router_2*) connected via IP backbone (*Internet*), an 10BaseT access LAN, which supports up to 50 workstations (*LAN_50*) and two types of traffic sources: data and voice. The data traffic includes traffic from FTP, HTTP, e-mail, and print applications. VoIP traffic is generated as two telephonic conversations: one between *Telefon_1* and *Telefon_2*, and another between *Telefon_3* and *Telefon_4*.

The configuration of the network model ensures *Interactive Voice* type of service for VoIP traffic, based on Integrated Service QoS mechanism. The queuing scheme used in evaluations is WFQ (Weighted Fair Queuing). The main interest in this evaluation was to find how much the voice packetization interval influences the network load (the used throughput) for each coding scheme. Therefore, the simulation studies cover a broad range of voice encoders: G.711, G.723.1, G.726, G.278, and G.729 from ITU-T and GSM from ETSI. The performance for all coding schemes and packet sizes from 4 ms to

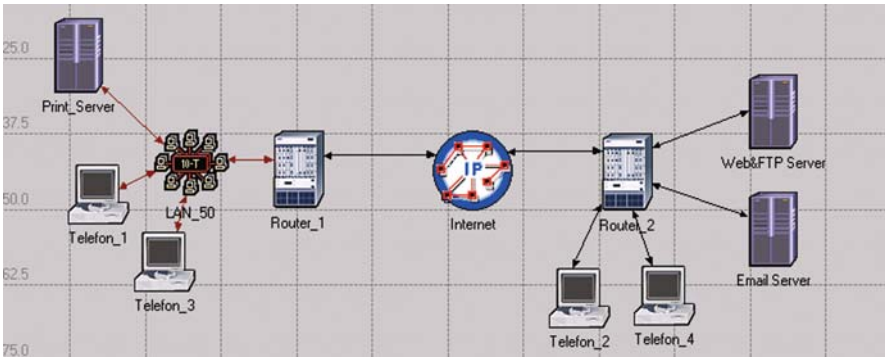

Fig. 3.24 Network model in IT Guru OPNET

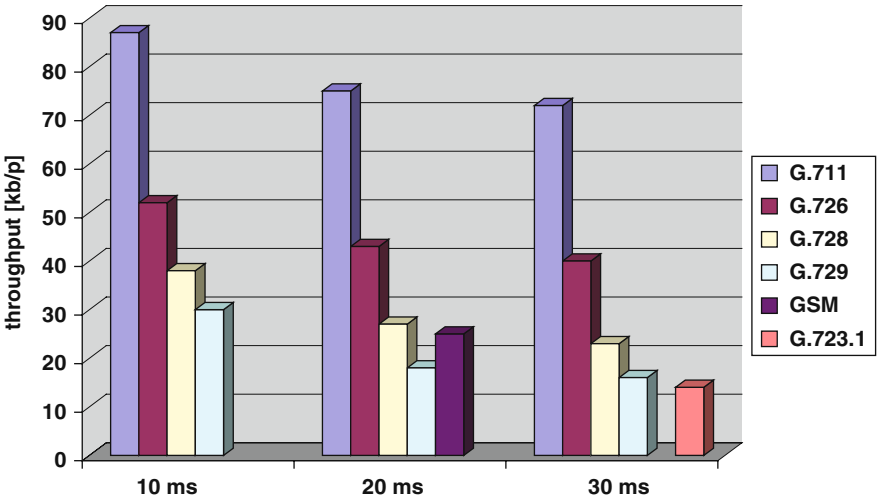

Fig. 3.25 Network load for different coding scheme and packet sizes

30 ms was evaluated. The packetization interval is restricted by the standard to 20 ms for ETSI GSM and to 30 ms for ITU-T G.723.1.

The evaluation results shown in Fig 3.25 reveal not only high network loads for voice encoders at high bit rates, such as G.711 and G.726, but also little gain due to an increased packetization interval. The best performance, a network load five times lower than the reference one, we obtained for ITU-T G.723.1 and G.729 voice encoders. Such an improvement of the network load was encountered at packetization intervals greater than 10 ms.

In search of a good trade-off between efficient network utilization and high voice quality, it was observed that little differences appear in the performance for the same coding scheme when increasing the packetization interval from 20 to 30 ms. Thus, it can be concluded that from the evaluated coding schemes, the ITU-T G.729 coding scheme is the most appropriate compromise.

3.5 Coverage Planning for Fixed BWA Networks

The provision of Internet access and broadband multimedia services to residential users via wireless communication systems attracted an increasing interest of the research community, service providers, and the telecommunication industry. The WiMAX (Worldwide Interoperability for Microwave Access) specifications [WiMAX], which are a subset of IEEE 802.16 standard [802.16d], seem to be the winner for providing broadband wireless Internet access in urban, suburban, and rural environments with non–line-of-sight (NLoS) propagation. The Fixed WiMAX specification uses the OFDM 256 physical layer of the IEEE 802.16 standard to cope with expected channel impairments.

3.5.1 Coverage Planning for the 450-MHz Band

Frequency bands allocated for the WiMAX system are within the 2.5-GHz, 3.5-GHz, and 5.8-GHz spectrum with a maximum *effective isotropic radiated power* (EIRP) around 30 dBm. A maximum allowed guard time ratio of one fourth is specified to provide communication services with cell sizes from 1 km to 5 km in urban and suburban areas. However, the provision of Internet services in rural areas is limited to the *line-of-sight* (LoS) conditions when using the proposed frequency bands. For that reason, the WiMAX Forum is coordinating its efforts with world standard and regulatory bodies to propose the allocation of licensed and license-exempt spectrum in lower frequency bands. Of special interests are bands in sub–1-GHz frequency range that are currently allocated for analogue TV transmission and will be released as soon as analogue TV broadcast moves to digital terrestrial television. Frequency bands of interest are from 700 to 800 MHz. Another frequency band of interest at 450 MHz is currently occupied by analogue mobile telecommunication systems like *Nordic Mobile Telephone* (NMT), which are slowly dying out. WiMAX systems at 3.5 GHz and 450 MHz are compared by analyzing the coverage area against the radio signal level and the system capacity [TD(06)048, Hro06].

The WiMAX Forum proposed a modified Erceg model [Erc99, Erc01] for computing the path loss for selected transmission frequency bands. It has been implemented in software tool [Hro04] and applied to estimate the WiMAX coverage at 3.5 GHz. The Erceg path loss model has been initially designed for suburban areas, receiver antenna heights close to 2 m, base station heights between 10 and 80 m, and for frequency bands at 1.9 GHz. The model distinguishes three different terrain types: Terrain type A is a hilly terrain with moderate-to-heavy tree density and associated with the highest path loss; Terrain type B is characterized as either a mostly flat terrain with moderate-to-heavy tree densities or hilly terrain with light tree densities; Terrain type C is a flat terrain with light tree densities, producing the lowest path loss. A correction term for higher frequencies and receiver antenna heights was added to extend the validity of the model.

The Erceg model is not suitable for radio coverage calculation in rural and urban areas at 450 MHz. Instead, the Longley-Rice model is widely accepted for this frequency band in rural areas, and the conventional Okumura Hata model is appropriate for urban areas. The Longley-Rice model is a general-purpose propagation model, valid for frequency bands from 20 MHz and 40 GHz and path length between 1 km and 2000 km. It allows for computing the terrain roughness and radio horizons from digital elevation models of the terrain. Other parameters used in the model like average climate conditions and soil conductivity have to be set according to the base station location. The *Terrain Analysis Program* (TAP) [SOFT] has been applied to determine the radio coverage at 450 MHz.

The coverage of the WiMAX radio signal at different carrier frequencies (i.e., the maximum cell size) depends on terrain (rural, urban); transmitter properties like transmit power, antenna radiation pattern, antenna tilt, and so forth; and receiver characteristics like receiver sensitivity, receiver antenna pattern, receiver noise figure, and so forth. In order to obtain results independent of transmitter antenna characteristics and precise receiver implementation, the cell size is determined according to the *effective radiated power* (ERP) at the transmitter and the receiver sensitivity expressed as electrical field strength. A typical receiver sensitivity varying from 30 dBμ to 15 dBμ was calculated for off-the-shelf antennas for 3.5 GHz and 450 MHz frequency bands according to the receiver sensitivity specified by WiMAX Forum for the most robust modulation and coding scheme. The probability of terrain coverage is set to 95%. The subscriber station height is set to 7 m above ground level.

In flat rural areas and with receiver sensitivity of 25 dBμ, the average cell radius at 450 MHz is 20 km, whereas at 3.5 GHz it is 10 km. An example of cell sizes for a flat rural area at 450 MHz and 3.5 GHz is presented in Fig. 3.26. The impact of frequency band on cell size is less than expected from free-space calculations, as the cell size is limited by Earth curvature and terrain irregularities like small hills in the rural flat area. Whereas in a hilly rural area the estimated cell size at 450 MHz is 15 km, it is only 1 km at 3.5 GHz, which clearly leads to the conclusion that the 3.5 GHz can be an inappropriate frequency band for certain hilly rural terrains. Furthermore, at 3.5 GHz reflections from geographic obstacles, like hills and mountains, do not significantly contribute

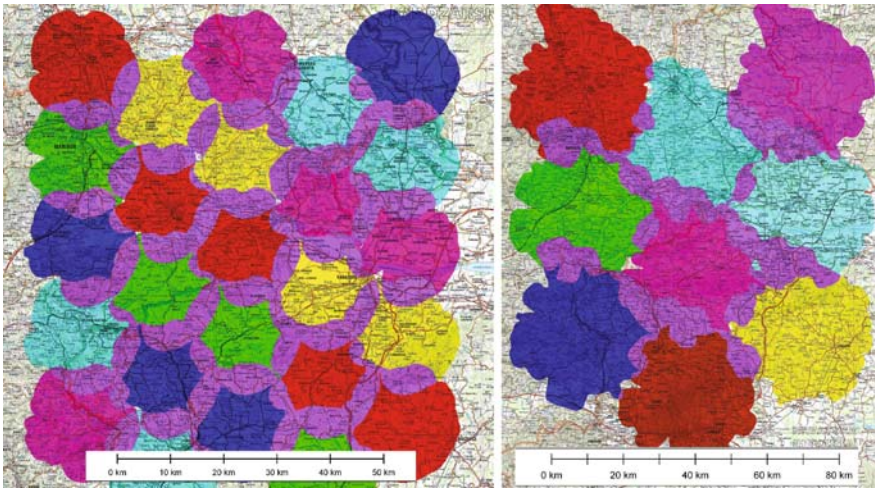

(a) 3.5 GHz **(b)** 450 MHz

Fig. 3.26 WiMAX cellular coverage for flat rural area (copyright © 2006 Softcom [Jav06])

to the received power due to terrain roughness, whereas at 450 MHz reflections from hills may improve the radio coverage.

In urban areas, the assumption is made that the subscriber station is placed inside buildings, which requires 5 dB additional electrical field strength. Because of this requirement and propagation conditions, the cell radius shortens to 2 km and 3 km for carrier frequencies of 3.5 GHz and 450 MHz, respectively. The Okumura path loss model was applied to obtain cell size at the lower frequency band. The difference between the cells sizes is not significant, which is explained by the occurrence of reflection and diffraction in urban areas.

In urban and flat rural areas, both analyzed frequency bands can be applied for radio coverage, whereas in hilly rural area, the WiMAX system operating at 450 MHz clearly outperforms the one at 3.5 GHz.

3.5.2 A WiMAX Deployment Example

This section presents insights gained from a radio network planning process with the objective to install a WiMAX *point-to-multipoint* (PtM) wireless network covering the district of Covilhã with 550 km^2, and in particular the city area in detail. The final aim was to guarantee a PtM connection from the Health Science Faculty of the University of Beira Interior (HSF/UBI) located in Covilhã to the whole city center.

3.5.2.1 The Planning Process

In WiMAX networks, interference limits frequency reuse, and coverage is limited by noise and interference. Accordingly, the process of cellular planning has to simultaneously account for *carrier-to-noise* (C/N) and *carrier-to-interference* (C/I) constraints. For coverage calculations, a simple propagation model [Rap02] was employed where different propagation environments are modeled by their propagation exponents γ with $\gamma = 2$ for free-space propagation in rural areas, $\gamma = 3$ for urban areas without shadowing, and $\gamma = 4$ for shadowed urban areas. Let us consider an example with a total antenna gain (transmit and receive) of 19 dBi, a transmit power of 2 dBW, a bandwidth of 3.5 MHz, and a noise factor of 3 dB. Figure 3.27 shows the obtained C/N values. C/N requirements $(C/N)_{min}$ of the order 6 to 8 dB can only be achieved for $\gamma = 2$ and $\gamma = 3$; for $\gamma = 3$ even only for distances up to 6 km. Note that typical C/N requirements for higher-order modulations schemes are about 15 to 16 dB [802.16d, 802.16e]). The conclusion from these considerations is that coverage is not a limitation in rural areas with free-space propagation. In urban areas, however, large coverage areas will be impossible, and cells with a maximum radius up to 3 to 4 km have to be used.

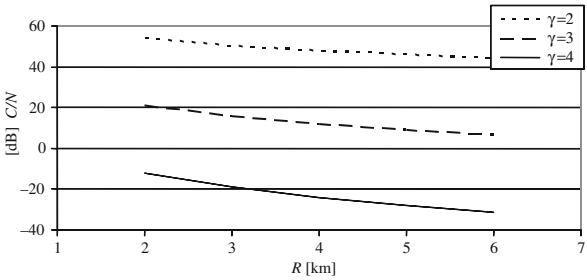

Fig. 3.27 Carrier-to-noise ratio for different propagation environments and $f = 3.5$ GHz (rain attenuation is included)

In order to improve C/I values, the benefits of 180° sector antennas with several re-use patterns were investigated. Figure 3.28 shows the obtained results for urban areas without shadowing. By sectorization, the minimum re-use pattern of 4 to 7 for omnidirectional antennas could be reduced to 3. As a conclusion, sectorization will be used in the urban area of Covilhã while omnidirectional cells with a planned coverage radius of about 3 km are used for covering the district of Covilhã [Vel06b, TD(07)017].

Up to now, the coverage estimations relied on a simple propagation model. In the following, LoS discovery will be enabled for a better cellular planning by incorporating *Geographic Information Systems* (GIS) functionalities. Figure 3.29 shows the LoS areas for the district of Covilhã. Considering a cell radius of 3 km leads to the 18 sites (3 with 180° sectorization) marked by dark dots. A LoS coverage of about 70% is obtained by using digital terrain models and ArcGIS 9.0 [Ran02] (3D Analyst extension). In villages, towns, and cities, the LoS coverage is even 83% guaranteeing propagation exponents of $\gamma = 2$ in rural

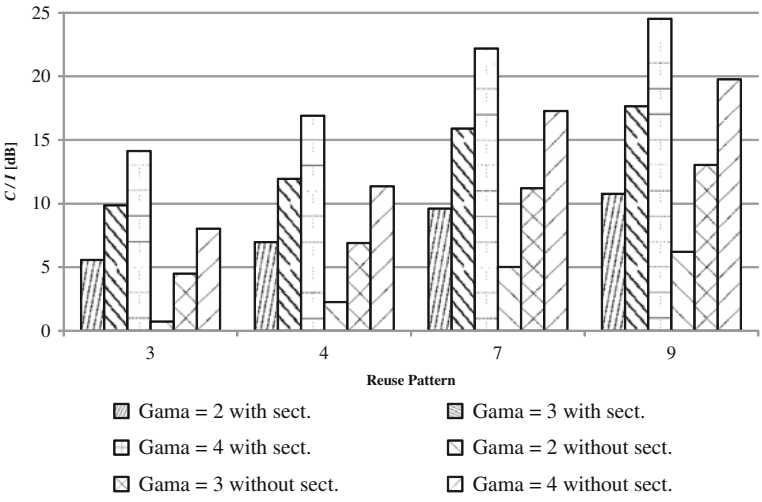

Fig. 3.28 Carrier-to-interference ratio with omnidirectional and sectorial antennas in different environments

Fig. 3.29 LoS discovery for the district of Covilhã (copyright © 2006 Springer [Vel06b])

areas and $\gamma = 3$ in dense urban areas. The frequency re-use layout and a scheme for the wireless backhaul network can be found in [TD(07)017, Vel06a, Vel06b].

3.5.2.2 Practical Experience with WiMAX Deployment

After the planning phase, a first network with *point-to-points* (PtP) links was installed. In Covilhã, two buildings with less than 2 km distance are connected by a BreezeNET B100 [BreezeN] PtP link operating in the 5.4-GHz band. A connection to Castelo Branco was established by using two relays, one located in Gardunha and one in Castelo Branco, leading to a three-hop solution with links of 22.5 km, 28.5 km, and 1 km.

Additionally, cellular coverage in Covilhã was achieved by installing BreezeMAX [BreezeM] equipment in the Health Sciences Faculty. Field tests were performed with the *outdoor radio unit* (ODU) operating at 3551.75 MHz (downlink) and 3451.75 MHz (uplink). The ODU transmitter power is 28 dBm. The results obtained from these field trials included signal-to-noise ratios and throughputs along major streets. As a conclusion, from more than 1400 measurements, a propagation exponent of $\gamma = 2.33$ was found as valid for the modified Friis model. A graphical presentation of the results can be found in [TD(07)047, Mar07].

Fig. 3.30 LoS discovery for the installed cell

LoS discovery was also performed for the installed cell by using GIS. Figure 3.30 shows the obtained results (by using a 10 dBi omnidirectional antenna with a 9° elevation). The corresponding geographic distribution of the supported modulation and coding schemes can be found in [Vel07b].

For the WiMAX cellular coverage of the whole region of Beira Interior, Portugal, many combinations of the placement of BSs and types of antennas can be explored. By using GIS for cellular planning purposes, one specific exercise compared the use of omnidirectional antennas with the use of sectorized ones on the whole region [TD(07)047, Mar07]. The advantages of using the latter in terms of interference mitigation are clear because the area of interference is reduced from 36.4% in the omnidirectional case down to 0.3% when sectorization is used, while increasing substantially the covered area (see Table 3.4).

There is a strong need of using sector antennas to guarantee an adequate coverage and interference mitigation. The need for LoS connection to guarantee good-quality communications was verified during PtM field trials. It confirms the need of an adequate LoS dimensioning. Extra details on the GIS-based cellular planning tools can be found in [Seb07].

Table 3.4 Coverage and interference areas in the second exercise for the whole region of Beira Interior

Type of Antenna	Covered Area (%)	Area of Interference (%)	Noncovered Area (%)
Omnidirectional	50.8	36.4	12.8
Sectorial	86.9	0.3	12.8

References

[OPNET] OPNET IT Guru Homepage, http://www.opnet.com/services/university/itguru_academic_edition.html.
[SOFT] Softwright LLC, http://www.softwright.com.
[BreezeN] Alvarion BreezeNET B100, http://www.alvarion.com/products/breezenet_b/.
[BreezeM] Alvarion BreezeMAX, http://www.alvarion.com/products/BrrezeMAX/.
[SEA] IST project SEACORN Simulation of Enhanced UMTS Access and Core Networks, http://seacorn.ptinovacao.pt/.
[ANSI] ANSI T1.801.03, American National Standard for Telecommunications – Digital Transport of One-Way Video Signals. Parameters for Objective Performance Assessment, American National Standards Institute, 2003.
[25.214] 3GPP, 3GPP TS 25.214 Physical Layer Procedures (FDD), December 2006.
[25.309] 3GPP, 3GPP TS 25.309 V6.4.0 FDD Enhanced Uplink; Overall Description; Stage 2, June 2005.
[26.234] 3GPP, 3GPP TS 26.234 End-to-End Transparent Streaming Service; Protocols and Codecs, June 2007.
[802.16d] IEEE, IEEE802.16-2004: IEEE Standard for Local and Metropolitan Area Networks Part 16: Air Interface for Fixed Broadband Wireless Access Systems, October 2004.
[802.16e] IEEE, IEEE802.16e-2005: IEEE Standard for Local and Metropolitan Area Networks Part 16: Air Interface for Fixed and Mobile Broadband Wireless Access Systems, Amendment 2: Physical and Medium Access Control Layers for Combined Fixed and Mobile Operation in Licensed Bands, February 2006.
[G.107] ITU-T Recommendation G.107: The E Model, A Computation Model for Use in Transmission Planning, International Telecommunication Union, 2005.
[G.108] ITU-T Recommendation G.108: Application of the E-model: A Planning Guide, International Telecommunication Union, 2001.
[H.264] ITU-T Recommendation H.264: Advanced Video Coding for Generic Audiovisual Services, International Telecommunication Union, March, 2003.
[P.862] ITU-T Recommendation P.862: Perceptual Evaluation of Speech Quality (PESQ), An Objective Method for End-to-End Speech Quality Assessment of Narrowband Telephone Networks and Speech Codecs, International Telecommunication Union, February 2002.
[P.910] ITU-T∼Recommendation P.910, Subjective Video Quality Assessment Methods for Multimedia Applications, International Telecommunication Union, September 1999.
[WiMAX] Worldwide Interoperability for Microwave Access (WiMAX) Forum, http://www.wimaxforum.org.
[RFC3448] M. Handley, S. Floyd, J. Padhye, and J. Widmer, TCP Friendly Rate Control (TFRC): Protocol Specification, IETF RFC3448, January 2003.
[And00] J. Andersson, M. Kihl, D. Söbirk, Overload xontrol of a parlay X application server, SCS Symposium on Performance Evaluation of Computer and Telecommunication Systems (SPECTS), 2000.
[And04] J. Andersson, M. Kihl, Load balancing and admission control of a parlay X application server, Nordic Teletraffic Seminar, 2004.
[And05a] J. Andersson, C. Nyberg, Shaping in multi service architectures, Swedish National Computer Networking Workshop, 2005.
[And05b] J. Andersson, P. Zeephongsekul, Shaping variables in service level agreements at application level, IEEE International Symposium on Modeling, Analysis, and Simulation of Computer and Telecommunication Systems (MASCOTS), 2005.
[And06] J. Andersson, C. Nyberg, M. Kihl, Traffic shaping and dimensioning of an external overload controller in service architectures, IEEE Conference on Local Computer Netowrks (LCN), 2006.
[Ant07a] P. Antoniou, V. Vassiliou, A. Pitsillides, Delivering adaptive scalable video over the wireless internet, ERCIM Workshop on eMobility, 2007.

[Ant07b] P. Antoniou, A. Pitsillides, V. Vassiliou, Adaptive feedback algorithm for internet video streaming based on fuzzy rate control, IEEE Symposium on Computers and Communications (ISCC), 2007.
[Ber02] F. Berggren, R. Jäntti, Asymptotically fair scheduling on fading channels, IEEE Vehicular Technology Conference (VTC Spring), 2002.
[Ber03] F. Berggren, R. Jäntti, Multiuser scheduling over Rayleigh fading channels, IEEE Globecom, 2003.
[Ber04] J. L. van den Berg, R. Litjens, J. Laverman, HSDPA flow level performance: The impact of key system and traffic aspects, ACM International Symposium on Modeling, Analysis and Simulation of Wireless and Mobile Systems (MSWiM), 2004.
[Ber06] F. Berggren, R. Litjens, Performance analysis of access selection and transmit diversity in multi-access networks, International Conference on Mobile Computing and Networking (Mobicom), 2006.
[Ber91] W. Berger, Comparison of Call Gapping and Percent Blocking for Overload Control in Distributed Switching Systems and Tele-communications Networks, IEEE Transactions on Communications, Vol. 39, pp. 574–580, 1991.
[Bik06] A. Bikfalvi, P. Patras, C. M. Vancea, V. Dobrota, The Management infrastructure of a network measurement system for QoS parameters, International Conference on Software, Telecommunications & Computer Networks (SOFTCOM), 2006
[Boh07a] T. M. Bohnert, E. Monteiro, Multi-class measurement based admission control for a QoS framework with dynamic resource management, Journal of Network and Systems Management, Vol. 15, No. 2, pp. 219–240, June 2007.
[Boh07b] T. M. Bohnert, E. Monteiro, Y. Koucheryavy, D. Motchanov, Nonparametric and self-tuning measurement-based admission control, IFIP Networking, 2007.
[Boh08] T. M. Bohnert, D. Staehle, G. S. Kuo, Y. Koucheryavy, E. Monteiro, Speech quality aware downlink admission control for fixed IEEE 802.16 Wireless MAN, IEEE International Conference on Communications (ICC), 2008.
[Bon03a] T. Bonald, A. Proutière, Wireless downlink data channels: User performance and cell dimensioning, International Conference on Mobile Computing and Networking (Mobicom), 2003.
[Bon03b] T. Bonald, A. Proutière, Insensitive bandwidth sharing in data networks, Queuing Systems, Vol. 44, pp. 69–100, 2003.
[Bor03] S. C. Borst, User-level performance of channel-aware scheduling algorithms in wireless data networks, IEEE INFOCOM, 2003.
[Bou04] J-Y. Boudec, P. Thiran, NETWORK CALCULUS A Theory of Deterministic Queuing Systems for the Internet, LNCS 2050, Springer, 2001.
[Bro04] F. Brouwer, I. de Bruin, J. de Bruin, N. Souto, F. Cercas, A. Correia, Usage of link-level performance indicators for HSDPA network-level simulations in E-UMTS, IEEE International Symposium on Spread Spectrum Techniques and Applications, 2004.
[Cab06a] O. Cabral, F. J. Velez, C. Franco, R. Rei, Urban cellular planning optimisation of multi-service enhanced UMTS based in economic issues, International Conference on Wired/Wireless Internet Communications (WWIC), 2006.
[Cab06b] O. Cabral, F. J. Velez, G. Hadjipollas, M. Stylianou, J. Antoniou, V. Vassiliou, A. Pitsillides, Enhanced UMTS simulation-based planning in office scenarios, European Wireless, 2006.
[Cab06c] O. Cabral, F. J. Velez, G. Hadjipollas, M. Stylianou, J. Antoniou, V. Vassiliou, A. Pitsillides, Enhanced UMTS cellular planning for multiple traffic classes in offices scenarios, IEEE International Symposium on Personal, Indoor and Mobile Radio Communications (PIMRC), 2006.
[Cen98] S. Cen, C. Pu, J. Walpole, Flow and congestion control for internet media streaming applications, SPIE/ACM Multimedia Computing and Networking, 1998.
[Cla01] A. Clark, Modeling the effects of burst packet loss and recency on subjective voice quality, IP Telephony Workshop, 2001.

[Com84] R. A. Comroe, D. J. Costello, Jr., ARQ schemes for data transmission in mobile radio systems, IEEE Journal of Selected Areas in Communications, Vol. 2, No. 4, July 1984.
[Der06] J. Derksen, R. Jansen, M. Maijala, E. Westerberg, HSDPA performance and evolution, Ericsson Review, No. 3, 2006.
[Dim05] A. Dimou, O. Nemethova, M. Rupp, Scene change detection for H.264 using dynamic threshold techniques, EURASIP Conference on Speech and Image Processing, Multimedia Communications and Service, 2005.
[Erc99] V. Erceg, L. J. Greenstein, S. Y. Tjandra, S. R. Parkoff, A. Gupta, B. Kulic, A. A. Julius, R. Bianchi, An empirical based path loss model for wireless channels in suburban environments, IEEE Journal on Selected Areas in Communications, Vol. 17, No. 7, pp. 686–687, July 1999.
[Erc01] V. Erceg, et al., Channel models for fixed wireless applications, IEEE 802.16a Working Group Document 802.16a-03/01, January 2001.
[Eva99] J. Evans, D. Everitt, On the teletraffic capacity of CDMA cellular networks, IEEE Transactions on Vehicular Technology, Vol. 48, No. pp. 153–165, January 1999.
[Fer05] J. Ferreira, F.J. Velez, Enhanced UMTS services and applications characterisation, Telektronikk, Vol. 101, No. 1, pp. 113–131, 2005.
[Fur02] A. Furuskär, S. Parkvall, M. Persson, M. Samuelsson, Performance of WCDMA high speed packet data, IEEE Vehicular Technology Conference (VTC Spring), 2002.
[Haj98] B. Hajek, L. He, On variations of queue response for inputs with the same mean and autocorrelation function, IEEE/ACM Trans. Networking, Vol. 6, No. 5, pp. 588–598, October 1998.
[Hil00] K. Hiltunen, R. de Bernardi, WCDMA downlink capacity estimation, IEEE Vehicular Technology Conference (VTC Spring), 2000.
[Hol06a] H. Holma, A. Toskala, 3GPP release 5 HSDPA measurements, IEEE International Symposium on Personal, Indoor and Mobile Radio Communications (PIMRC), 2006.
[Hol06b] H. Holma, A. Toskala, HSDPA/HSUPA for UMTS High Speed Radio Access for Mobile Communications, Wiley & Sons, New York, 2006.
[Hro06] A. Hrovat, T. Javornik, S. Plevel, R. Novak, T. Celcer, I. Ozimek, Comparison of WiMAX field measurements and empirical path loss model in urban and suburban environment, WSEAS Intternational Conference on Communications, 2006.
[Jac98] S. Jacobs, A. Eleftheriadis, Streaming video using dynamic rate shaping and TCP congestion control, Journal of Visual Communication and Image Representation, Vol. 9, No. 3, pp. 211–222, September 1998.
[Jav05] T. Javornik, M. Mohorcic, A. Svigelj, I. Ozimek, G. Kandus, Adaptive coding and modulation for mobile wireless access via high altitude platforms, Wireless Personal Communications, Vol. 32, No. 3–4, pp. 301–317, February 2005.
[Jav06] Tomaž Javornik, Gorazd Kandus, Andrej Horvat, Igor Ozimek, Comparison of WiMAX Coverage at 450MHz and 3.5GHz, Softcom, Split/Dubrovnik, Croatia, 2006.
[Joh06] C. John, Effect of Content on Perceived Video Quality, Univ. of Colorado Interdisciplinary Telecommunications Program: TLEN 5380 – Video Technology, August 2006.
[Jua06] J. M. Juárez Valero, R. R. Paulo, F. J. Velez, Tele-traffic simulation for mobile communication systems beyond 3G, Advanced International Conference on Telecommunications (AICT), 2006.
[Jua07] J. M. Juárez Valero, R. R. Paulo, F. J. Velez, Event-based simulation for multi-rate multi-service traffic validation in B3G systems, IEEE Vehicular Technology Conference (VTC Spring), 2007.
[Jur07] M. Jurvansuu, J. Prokkola, M. Hanski, P. Perälä, HSDPA performance in live networks, IEEE International Conference on Communications (ICC), 2007.
[Kaj04] A. Kajackas, V. Batkauskas, A. Medeisis, Individual QoS rating for voice services in cellular networks, IEEE Communications Magazine, pp. 88–93, June 2004.
[Kaj06] A. Kajackas, D. Gursnys, Investigation of voice frame erasures in GSM, Electronics and Electrical Engineering, Vol. 4. p. 47–53, 2006.

[Kon80] A. Konheim, A queueing analysis of two ARQ protocols, IEEE Transactions on Communications, Vol. 28, No. 7, pp. 1004–1014, July 1980.
[Kou05] H. Koumaras, A. Kourtis, D. Martakos, Evaluation of video quality based on objectively estimated metric, Journal of Communications and Networking, Vol. 7, No. 3, September 2005.
[Kus05] T. M. Kusuma, H. J. Zepernick, M. Caldera, On the development of a reduced-reference perceptual image quality metric, Systems Communications (ICW), 2005.
[Lei07] J. Leino, A. Penttinen, J. Virtamo, Flow-optimized random access for wireless mulithop networks, ACM International Symposium on Modeling, Analysis and Simulation of Wireless and Mobile Systems (MSWiM), 2007.
[Lai06] J. Laiho, A. Wacker, T. Novosad, Radio Network Planning and Optimisation for UMTS, John Wiley & Sons Ltd., New York, 2006.
[Lem04] J. Lempiäinen, M. Manninen, UMTS Radio network Planning, Optimization, and QoS Management, Kluwer Academic Publishers, Dordrecht, 2004.
[Lev06] R. Levering, M. Cutler, The Portrait of a Common HTML Web Page, ACM Symposium on Document engineering, (DoEng), 2006.
[Li97a] S.-Q. Li, C.-L. Hwang, Queue response to input correlation functions: discrete spectral analysis, IEEE Transactions on Networking, Vol. 1, No. 5, pp. 522–533, October 1993.
[Li97b] S.-Q. Li, C.-L. Hwang, On the convergence of traffic measurement and queuing analysis: a statistical-matching and queuing (SMAQ) tool, IEEE/ACM Trans. Networking, Vol. 5, No. 1, pp. 95–110, February 1997.
[Lov01] R. Love, A. Ghosh, R. Nikides, L. Jalloul, M. Cudak, B. Classon, High speed downlink packet access performance, IEEE Vehicular Technology Conference (VTC Spring), 2001.
[Lut91] E. Lutz, D. Cygan, N. Dippold, F. Dolainsky, W. Papke, The land mobile satellite channel-recording, statistics and channel model, IEEE Transactions on Vehicular Technology, Vol. 40, pp. 375–386, May 1991.
[Mäd06] A. Mäder, D. Staehle, An analytical model for best effort traffic over the UMTS enhanced uplink, IEEE Vehicular Technology Conference (VTC Fall), 2006.
[Mäd07] A. Mäder, D. Staehle, A flow-level simulation framework for HSDPA-enabled UMTS networks, ACM International Symposium on Modeling, Analysis and Simulation of Wireless and Mobile Systems (MSWiM), 2007.
[Mar07] M. Marques, J. Ambrósio, C. Reis, D. Gouveia, D. Robalo, F. J. Velez, R. Costa, J. Riscado, Design and planning of IEEE 802.16 networks, IEEE International Symposium on Personal, Indoor and Mobile Radio Communications (PIMRC), 2007.
[Mir05] S. Mirtchev, I. Stanev, Evaluation of a single server delay system with a generalized poisson input stream, International Teletraffic Congress (ITC), 2005.
[Mir06] S. Mirtchev, Palm's machine-repair model with a generalised Poisson input stream and constant service time, International Conference on Software, Telecommunications and Computer Networks (SOFTCOM), 2006.
[Mir07] S. Mirtchev, Study of queueing systems with state dependent mean service time, International Symposium on Radio Systems and Space Plasma, 2007
[Molxx] D. Moltchanov, Y. Koucheryavy, J. Harju, Cross-layer modeling of wireless channels for data-link and IP layer performance evaluation, Computer Communications, Vol. 29, No. 7, pp. 827–841, April, 2006.
[Mol05] D. Moltchanov, Y. Koucheryavy, J. Harju, Non-preemptive ΣD-BMAP/D/1/K queuing system modeling the frame transmission process over wireless channels, International Teletraffic Congress (ITC), 2005.
[Mar02] P. Marziliano, F. Dufaux, S. Winkler, T. Ebrahimi, A no-reference perceptual blur metric, IEEE International Conference on Image Processing, 2002.
[Nec05] M. C. Necker, A simple model for the IP packet service time in UMTS networks, International Teletraffic Congress (ITC), 2005.

[Nec06] M. C. Necker, A comparison of scheduling mechanisms for service class differentiation in HSDPA networks, AEÜ International Journal of Electronics and Communications, Vol. 60, No. 2, pp. 136–141, 2006.

[Nem04] O. Nemethova, M. Ries, E. Siffel, M. Rupp, Quality assessment for H.264 coded low-rate and low-resolution video sequences, IASTED International Conference on Communications, Internet, and IT (CIIT), 2004.

[Ong03] E. P. Ong, W. Lin, Z. Lu, S. Yao, X. Yang, F. Moschetti, Low bitrate quality assessment based on perceptual characteristics, International Conference on Image Processing (ICIP), 2003.

[Par05] S. Parkvall, J. Peisa, J. Torsner, M. Sagfors, P. Malm, WCDMA enhanced uplink – principles and basic operation, IEEE Vehicular Technology Conference (VTC Spring), 2005.

[Pin04] M. H. Pinson, S. Wolf, A new standardized method for objectively measuring video quality, IEEE Transactions on Broadcasting, Vol. 50, No. 3, pp. 312–322, September 2004.

[Raa06] A. Raake, Speech Quality of VOIP: Assessment and Prediction, John Wiley & Sons, New York, 2006.

[Ran02] S. Rana, J. Morley, Optimising visibility analyses using topographic features on the terrain, Centre for Advanced Spatial Analysis, University College London, London, UK, 2002.

[Rap02] T. S. Rappaport, Wireless Communications – Principles and Practice, Prentice Hall, Englewood Cliffs, NJ, 2002.

[Rej99] R. Rejaie, M. Handley, D. Estrin, RAP: An end-to-end rate-based congestion control mechanism for realtime streams in the internet, IEEE INFOCOM, 1999.

[Rie05] M. Ries, O. Nemethova, M. Rupp, Reference-Free Video Quality Metric for Mobile Streaming Applications, Internation Symposium on DSP and Communications System (DSPCS) and Workshop on the Internet, Telecommunications and Signal Processing (WITSP), 2005.

[Rie07a] M. Ries, O. Nemethova, M. Rupp, Motion based video quality estimation for H.264/AVC video streaming, International Symposium on Wireless Pervasive Computing, 2007.

[Rie07b] M. Ries, C. Crespi, O. Nemethova, M. Rupp, Content based video quality estimation for H.264/AVC video streaming, IEEE Wireless Communication & Networking Conference (WCNC), 2007.

[Rix99] A. W. Rix, A. Bourret, M. P. Hollier, Models of human perception, Journal of BT Tech., Vol. 17, No. 1, pp. 24–34, January 1999.

[Ros89] Z. Rosberg, N. Shacham, Resequencing delay and buffer occupancy under the selective-repeat ARQ, IEEE Transactions on Information Theory, Vol. 35, No. 1, pp. 166–173, January 1989.

[Ros03] M. Rossi, M. Zorzi, An accurate heuristic approach for UMTS RLC delay statistics evaluation, IEEE Vehicular Technology Conference (VTC Spring), 2003.

[Saw98] Y.-S. Saw, P. M. Grant, M. Hannah, A comparative study of nonlinear video rate control techniques: Neural networks and fuzzy logic, IEEE International Conference on Acoustics, Speech, and Signal Processing (ICASSP), 1998.

[Seb07] P. Sebastião, F. Velez, R. Tomé, R. Costa, D. Robalo, A. Grilo, A. Rodrigues, F. Cercas, User capacity based planning tool for Wi-Fi and WiMAX networks, WEIRD Workshop on WiMAX, Wireless and Mobility, 2007.

[Sip00] K. Sipilä, K.-C. Honkasalo, J. Laiho-Steffens, A. Wacker, Estimation of capacity and required transmission power of WCDMA downlink based on a downlink pole equation, IEEE Vehicular Technology Conference (VTC Spring), 2000.

[Smo07] M. Smolnikar, T. Javornik, M. Mohorcic, Channel decoder assisted adaptive coding and modulation for HAP communications, IEEE Vehicular Technology Conference (VTC Spring), 2007.

[Sta04] D. Staehle, A. Mäder, An analytic model for deriving the node-B transmit power in heterogeneous UMTS networks, IEEE Vehicular Technology Conference (VTC Spring), 2004.

[Sta05] D. Staehle, An analytic method for coverage prediction in the UMTS radio network planning process, IEEE Vehicular Technology Conference (VTC Spring), 2005.
[Sta07] D. Staehle, A. Mäder, A model for time-efficient HSDPA simulations, IEEE Vehicular Technology Conference (VTC Fall), 2007.
[Sun01] L. L. Sun, G. B. Wade, Lines, E. Ifeachor, Impact of packet loss location on perceived speech quality, IP Telephony Workshop (IPTEL), 2001.
[Tsa98] D. H. K. Tsang, B. Bensaou, S. T. C. Lam, Fuzzy based rate control for real-time MPEG video, IEEE Transactions on Fuzzy Systems, Vol. 6, No. 4, November 1998.
[Vas06] V. Vassiliou, P. Antoniou, I. Giannakou, A. Pitsillides, Requirements for the transmission of streaming video in mobile wireless networks, International Conference on Artificial Neural Networks (ICANN), 2006.
[Vee97] V. V. Veeravalli, A. Sendonaris, N. Jain, CDMA coverage, capacity and pole capacity, IEEE Vehicular Technology Conference (VTC), 1997.
[Vel06a] F. J. Velez, V. Carvalho, D. Santos, R. P. Marcos, R. Costa, P. Sebastião, A. Rodrigues, Aspects of cellular planning for emergency and safety services in mobile WiMax networks, International Symposium on Wireless Pervasive Computing (ISWPC), 2006.
[Vel06b] F. J. Velez, V. Carvalho, D. Santos, R. P. Marcos, R. Costa, P. Sebastião, R. Tomé, A. Rodrigues, Cellular planning of an IEEE 802.16 wireless metropolitan area network, International Conference on Telecommunications (ICT), 2006.
[Vel07a] F. J. Velez, N. Anastácio, F. Merca, O. Cabral, Cost/revenue optimisation of multiservice cellular planning for city centre E-UMTS, IEEE Vehicular Technology Conference (VTC Spring), 2007.
[Vel07b] F. J. Velez, P. Sebastião, Design and planning of WiMAX networks, Mobile WiMAX – Towards Ubiquitous Internet, Final Workshop of MobileMAN, 2007.
[Vit93] A. Viterbi, A. Viterbi, Erlang capacity of a power controlled CDMA system, IEEE Journal on Selected Areas in Communication, Vol. 11, pp. 892–893, August 1993.
[Vit94] A. Viterbi, A. Viterbi, E. Zehavi, Other-cell interference in cellular power controlled CDMA, IEEE Transactions on Communication, Vol. 42, pp. 1501–1504, February/March/April 1994.
[Win03] S. Winkler and F. Dufaux, Video quality evaluation for mobile applications, SPIE Conference on Visual Communications and Image Processing, Lugano, Switzerland, 2003.
[Win05] S. Winkler, Digital Video Quality, John Wiley & Sons, Chichester, England, 2005.
[Yan04] G. Yang, M. Gerla, M. Y. Sanadidi, Adaptive video atreaming in presence of wireless errors, IPIF/IEEE International Conference on Management of Multimedia Networks and Services (MMNS), 2004.
[Zor97] M. Zorzi, R. Rao, L. Milstein, ARQ error control for fading mobile radio channels, IEEE Transactions on Vehicular Technology, Vol. 46, No. 2, pp. 445–455, May 1997.

COST 290 documents can be downloaded from the link www.cost290.org. The COST 290 documents referenced in this chapter are listed below:

[TD(04)002] D. Staehle, A. Mäder, An Analytical Model for the Downlink Capacity of a UMTS Network.
[TD(05)006] J. Ferreira, F. Velez, Deployment Scenarios and Applications Characterization for Enhanced UMTS Simulation.
[TD(05)007] J. L. van den Berg, R. Litjens, J. Laverman, HSDPA Flow Level Performance: The Impact of Key System and Traffic Aspects.
[TD(05)008] D. Moltchnow, Y. Koucheryavy, J. Harju, Non-preemptive ΣD-BMAP/D/1/K Queuing System Modeling the Frame Transmission Process Over Wireless Channels.

[TD(05)014] M. Necker, A Simple Heuristic Model for the IP Packet Service Time Distribution in UMTS Networks.
[TD(05)015] J. Antoniou, V. Vassiliou, A. Pitsillides, Coverage and Capacity Planning for 3G and Beyond Mobile Networks.
[TD(05)034] S. Mirtchev, Evaluation of a Multi-server Delay System with a Generalized Poisson Input Stream.
[TD(05)037] M. Ries, O. Nemethova, M. Rupp, Reference-Free Video Quality Metric for Mobile Streaming Applications.
[TD(05)050] A. Kajackas, A. Anskaitis, D. Gursnys, L. Pavilanskas, Estimation of QoS Dynamics in the Wireless Networks.
[TD(05)051] O. Cabral, F.J. Velez, G. Hadjipollas, M. Stylianou, J. Antoniou, V. Vassiliou, A. Pitsillides, Enhanced UMTS Cost/Revenue Optimisation in Office Scenarios.
[TD(06)002] J. Andersson, C. Nyberg, M. Kihl, P. Zeephongsekul, Overload Control and Service Level Agreements in Service Architectures.
[TD(06)006] A. Mäder, D. Staehle, An Analytic Model for the Enhanced Uplink in UMTS.
[TD(06)017] J. M. J. Valero, R. R. Paulo, F. J. Velez, Tele-Traffic Simulation for Mobile Communication Systems Beyond 3G.
[TD(06)026] D. Staehle, On the Soft and Code Capacity of the UMTS Downlink.
[TD(06)027] F. Berggren, R. Litjens, Performance Analysis of Access Selection and Transmit Diversity in Multi-access Networks.
[TD(06)030] A. Kajackas, Speech Quality and Word-Level Intelligibility in Wireless. The Critical Impact of Lost Packets.
[TD(06)045] O. Cabral, F. J. Velez, C. Franco, R. Rei, Urban Cellular Planning Optimisation of Multi-service Enhanced UMTS Based in Economic Issues.
[TD(06)047] M. Ries, O. Nemethova, M. Rupp, Content Based Video Quality Estimation.
[TD(06)048] T. Javornik, G. Kandus, A. Hrovat, I. Ozimek, Comparison of WiMAX Coverage at 450 MHz and 3.5 GHz.
[TD(06)050] A. Bikfalvi, P. Patras, C. Mihai Vancea, V. Dobrota, The Management Infrastructure of a Network Measurement System for QoS Parameters.
[TD(07)001] D. Staehle, A. Mäder, An HSPDA Long-term Bandwidth Model.
[TD(07)007] S. Mirtchev, Study of Queueing System with State Dependant Mean Service Time.
[TD(07)009] E.-C. Popovici, T. Radulescu, Coding Scheme Impact on the IP-QoS Network Utilization and Voice Quality.
[TD(07)017] F. J. Velez, V. Carvalho, D. Santos, R. P. Marcos, R. Costa, P. Sebastião, R. Tomé, A. Rodrigues, Cellular Planning of an IEEE 802.16 Wireless Metropolitan Area Network.
[TD(07)019] G. Kandus, M. Smolnikar, T. Javornik, M. Mohorcic, Channel Decoder Assisted Adaptive Coding and Modulation for HAP Communications.
[TD(07)022] A. Penttinen, Flow-Optimized Random Access for Wireless Multihop Networks.
[TD(07)030] A. Anskaitis, Peculiarities Supporting of QoS at Edge of Cells.
[TD(07)031] Vasos Vasiliou, Delivering Scalable Video over the Wireless Internet.
[TD(07)046] F. J. Velez, N. Anastácio, F. Merca, O. Cabral, Cost/Revenue Optimisation of Multi-Service Cellular Planning for Business Centre E-UMTS.
[TD(07)047] Fernando Velez, Simulation of IEEE 802.11e in the context of interoperability.